古 脊 椎 动 物 学 报
VERTEBRATA PALASIATICA

DOI: 10.19615/j.cnki.2096-9899.210518

A new species of *Pteronisculus* from the Middle Triassic (Anisian) of Luoping, Yunnan, China, and phylogenetic relationships of early actinopterygian fishes

REN Yi[1,2,3] XU Guang-Hui[1,2*]

(1 *Key Laboratory of Vertebrate Evolution and Human Origins of Chinese Academy of Sciences*, *Institute of Vertebrate Paleontology and Paleoanthropology*, *Chinese Academy of Sciences* Beijing 100044
* Corresponding author: xuguanghui@ivpp.ac.cn)
(2 *CAS Center for Excellence in Life and Paleoenvironment* Beijing 100044)
(3 *University of Chinese Academy of Sciences* Beijing 100049)

Abstract Actinopterygii, the largest group of extant vertebrates, includes Cladistia, Actinopteri (Chondrostei plus Neopterygii) and closely related fossil taxa. The extinct genus *Pteronisculus* belongs to a stem lineage of actinopterygian fishes represented by 11 species from the Early Triassic of Madagascar, Europe and North America, and a single species from the early Middle Triassic of China. Here, we report the discovery of a new species of this genus, *Pteronisculus changae*, on the basis of five well-preserved specimens from the Middle Triassic (Anisian) marine deposits exposed in Luoping, eastern Yunnan, China. The discovery documents the second convincing species of *Pteronisculus* in the Middle Triassic and the largest stem actinopterygian fish in the Luoping Biota, having a maximum total length of up to 295 mm. The new species possesses a toothed lacrimal, which is characteristic of *Pteronisculus*, but it is easily distinguished from other species of the genus by some autapomorphies, e.g., a medial process at the middle portion of the intertemporal, 21 supraneurals, and 83 lateral line scales. The results of our cladistic analysis provide new insights into the relationships of early actinopterygians and recover *Pteronisculus* as a sister taxon of the Carboniferous rhadinichthyid *Cyranorhis* at the actinopterygian stem. Based on the body form, teeth and other features, it can be deduced that *Pteronisculus changae* is likely a relatively fast-swimming predator, feeding on planktonic invertebrates and smaller or younger fishes known to occur in the same biota. As one of the youngest species of the genus, the new species provides additional evidence to suggest that the diversity of *Pteronisculus* is higher than previously thought and that the eastern Paleotethys Ocean likely constituted a refuge for species of this genus during the early Middle Triassic.

Key words Luoping, Yunnan; Middle Triassic; *Pteronisculus*, Actinopterygii; phylogeny

Citation Ren Y, Xu G H, in press. A new species of *Pteronisculus* from the Middle Triassic (Anisian) of Luoping, Yunnan, China, and phylogenetic relationships of early actinopterygian fishes. Vertebrata PalAsiatica. DOI: 10.19615/j.cnki.2096-9899.210518

中国科学院战略性先导科技专项(B类) (编号：XDB 26000000, 18000000)、国家自然科学基金(批准号：41672001, 41688103)和中国科学院前沿科学重点研究项目(编号：QYZDB-SSW-DQC040)资助。

收稿日期：2021-01-28

1 Introduction

Actinopterygii (ray-finned fishes) is the most diverse clade of living vertebrates comprising Cladistia, Actinopteri (Chondrostei plus Neopterygii) and their closely related fossil taxa (Patterson, 1982; Gardiner, 1984; Coates, 1999; Hurley et al., 2007; Sallan, 2014; Friedman, 2015; Giles et al., 2017; Argyriou et al., 2018). The oldest proposed actinopterygian is the Early Devonian (~415 Ma) *Meemannia* on the basis of a few detached skull roofs and an isolated lower jaw (Zhu et al., 1999; Lu et al., 2016); even earlier candidates are represented by fragments subject to differing phylogenetic interpretations (Wang and Dong, 1989; Basden and Young, 2001; Schultze, 2015). The earliest widely accepted actinopterygian based on relatively complete specimens is the Middle Devonian (Eifelian, ~390 Ma) *Cheirolepis* spp. (Pearson and Westoll, 1979; Pearson, 1982; Arratia and Cloutier, 1996; Lu et al., 2016; Giles et al., 2017). There are so far 22 actinopterygian species (in 16 genera) recovered from the Devonian, according to our preliminary statistics. A greater diversification of actinopterygians occurred in the Carboniferous and Permian, with about 100 genera known from those periods (Gardiner, 1993; Lund and Poplin, 1997; Lund, 2000; Poplin and Lund, 2000, 2002; Bender, 2002, 2005; Figueiredo and Carvalho, 2004; Hamel, 2005; Mickle et al., 2009; Mickle, 2018; Wilson et al., 2018 and others). In the aftermath of the end-Permian mass extinction, neopterygians underwent a rapid radiation and basal actinopterygians (traditionally referred to the paraphyletic 'Palaeonisciformes') greatly declined and died out at the end of the Cretaceous (Friedman, 2015).

Pteronisculus is a basal actinopterygian genus with a geological range confined to Early to Middle Triassic. Until recently, 12 species were referred to the genus (Fig. 1A; Online Supplementary Material); among which there are four well-studied species based on relatively complete specimens: the Early Triassic *P. cicatrosus* (type species, Madagascar), *P. stensioi* (modified from *P. stensiöi*, according to the International Code of Zoological Nomenclature 32.5.2.1) and *P. magnus* (Greenland), and the Middle Triassic (Anisian) *P. nielseni* (South China). Although possible species of *Pteronisculus* were also reported from the late Permian (Lopingian) continental deposits of South Africa (Gardiner, 1966; Bender, 2004) and Early Triassic marine deposits of Alberta and British Columbia in Canada (Schaeffer and Mangus, 1976), they are based on poorly-preserved specimens and their reference to this genus is questionable (Romano et al., 2019). The relationships between *Pteronisculus* and other early actinopterygians are controversial; the genus has been recovered as either a stem actinopteran (Gardiner and Schaeffer, 1989; Xu and Gao, 2011; Xu et al., 2014a) or a stem actinopterygian (Giles et al., 2017; Argyriou et al., 2018). Additionally, the interrelationships between species of *Pteronisculus* have never been explored in a phylogenetic analysis.

Here, we report the discovery of a new species of *Pteronisculus* on the basis of five specimens from the Second Member of the Guanling Formation exposed near Dawazi village, Luoping Country in Yunnan Province (Fig. 1C). The specimens are nearly complete and well-

preserved in thinly laminated micritic limestone, permitting a detailed description of the morphology of the new species. The discovery documents the second species of *Pteronisculus* in South China (or more generally in Asia), and represents one of the youngest members of this genus, along with *P. nielseni* from the same fossil beds. A phylogenetic analysis was performed to resolve the interrelationships between *Pteronisculus* and other early actinopterygians.

In addition to the new species of *Pteronisculus* reported here, other macrofossils have been reported from the same fossiliferous horizons at the Luoping localities, including plants, invertebrates, diverse marine reptiles and other taxa of ray-finned fishes (Tintori et al., 2007, 2010; Sun et al., 2009, 2015, 2016; López-Arbarello et al., 2011; Wu et al., 2011; Xu and Wu, 2012; Feldmann et al., 2012; Wen et al., 2012, 2013, 2019; Xu and Ma, 2016; Xu and Zhao,

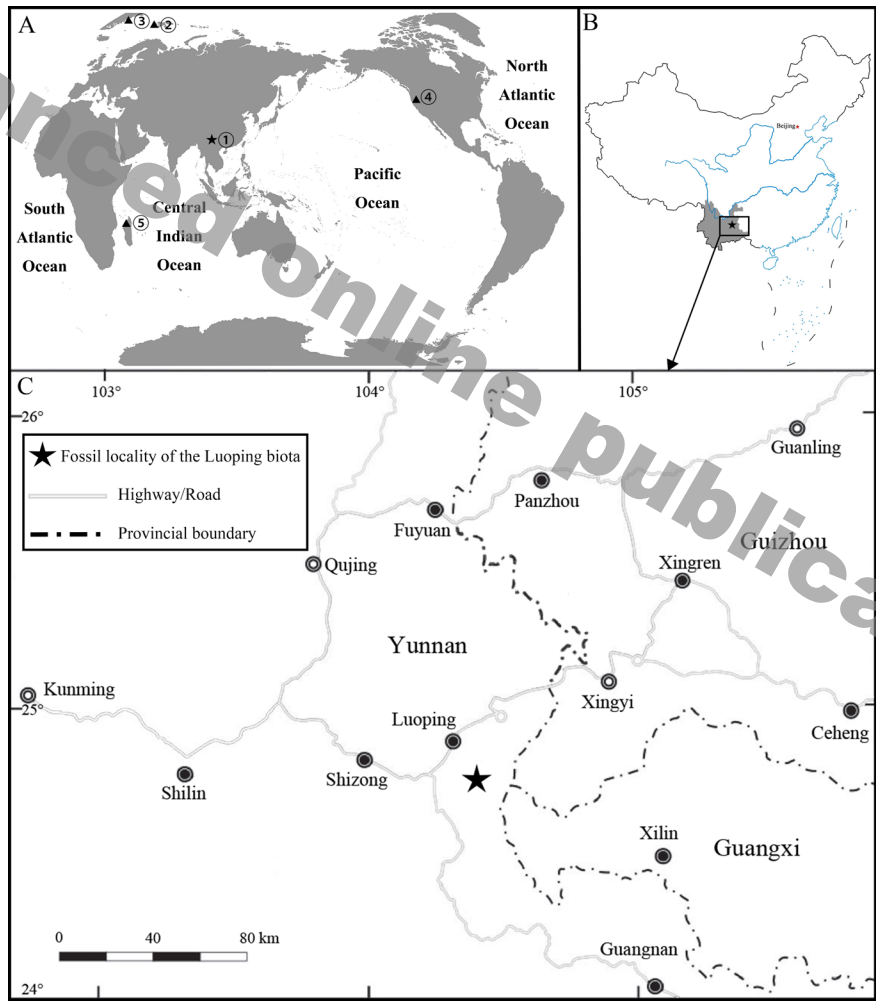

Fig. 1 Fossil localities of *Pteronisculus*

A. Map showing the global distribution of fossil localities of *Pteronisculus*: ① Yunnan, China, ② Spitsbergen (Svalbard), Norway ③ East Greenland, ④ Nevada, USA, ⑤ Madagascar; B. Geographic locality yielding *Pteronisculus changae* sp. nov. in Luoping, Yunnan, China; C. Map of eastern Yunnan showing the fossil locality (World map: GS(2016)No. 1611; China map: GS(2016)No. 1549)

2016; Xu et al., 2014a, b; Ma and Xu, 2017; Xu, 2020a). The whole of the fossil assemblage, known as the Luoping Biota, was suggested to have inhabited a semi-enclosed intraplatform basin (Hu et al., 2011; Benton et al., 2013). The age of this biota (Pelsonian, Anisian, ~244.2 Ma) is well constrained by conodont biozonation and zircon dating (Zhang et. al., 2009, 2015).

2 Material and methods

All specimens are housed in the fossil collections of the Institute of Vertebrate Paleontology and Paleoanthropology (IVPP), Chinese Academy of Sciences in Beijing, China. They were mechanically prepared with sharp steel needles. For better contrast, some specimens were dusted with ammonium chloride (NH4Cl) or immersed in water before being photographed. The relative positions of the fins and scale row counts follow Westoll (1944). The measurements of the specimens (Fig. 2) are as described in Schultze and Bardack (1987). The estimations of suspensorium angles are following Gardiner et al. (2005). The anatomical terms and bone names follow Gardiner and Schaeffer (1989), Grande and Bemis, 1998; Arratia, 2009 and Xu et al. (2014b).

A phylogenetic analysis was conducted by incorporating the new species of *Pteronisculus* into the matrix of Argyriou et al. (2018), which was in turn derived from that of Giles et al. (2017). Since the focus of this analysis is on the interrelationships of early actinopterygian clades above *Cheirolepis* level, we chose the basal sarcopterygian *Guiyu* as the outgroup, and removed other non-actinopterygians, as well as some actinopterygians based on incomplete or poorly preserved specimens (e.g., *Meemannia*, *Lawrenciella* and *Tanaocrossus*), and a few crown neopterygians (e.g., *Macrepistius*) from the data matrix. We added seven characters (Chars. 276–282), giving a total of 282 equally weighted characters coded for 67 taxa in our data matrix (Supplementary Material). Besides the new species of *Pteronisculus*, the additional taxa in the current data matrix include *Asialepidotus shingyiensis* (Su, 1959; Xu and Ma, 2018), *Ionoscopus cyprinoides* (Grande and Bemis, 1998; Maisey, 1999), *Louwoichthys pusillus* (Xu, 2021), *Ophiopsiella attenuata* (Wagner, 1863; Bartram, 1975; Lane and Ebert, 2015), *Pteronisculus cicatrosus* (Lehman, 1952), *P. magnus* (Nielsen 1942), *P. nielseni* (Xu

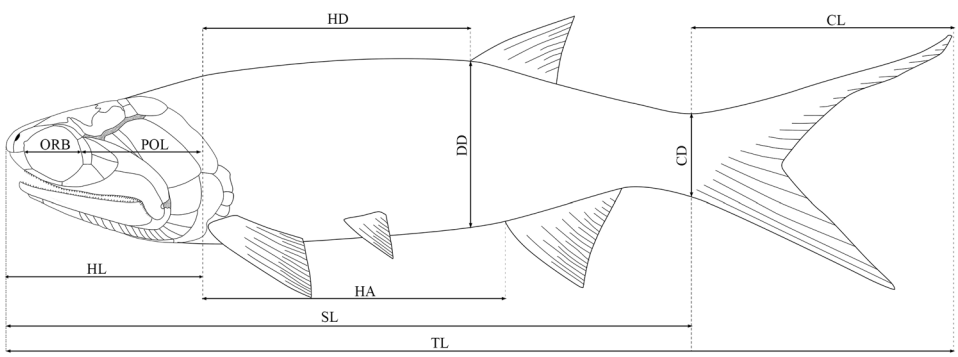

Fig. 2 Measurements adopted to describe the new species

et al., 2014b) and *Teffichthys madagascariensis* (Piveteau, 1934; Marramà et al., 2017). The maximum parsimony analyses were performed with a heuristic search in PAUP* v.4.0b10 using 500 random addition sequence replicates, holding five trees at each step, with the tree bisection and reconnection (TBR) strategy enabled and maxtrees set to automatically increase by 100.

Anatomical abbreviations an, anterior nostril; ang, angular; ao, antorbital; aop, antopercle; ar, articular; asp, ascending process of parasphenoid; bf, basal fulcrum; bpt, basipterygoid process; br, branchiostegal rays; cl, cleithrum; cla, clavicle; den, dentary; dhy, dermohyal; dpt, dermal palatine; dsp, dermosphenotic; ethc, ethmoid commissure canal; ff, fringing fulcra; fr, frontal; hll, horizontal longitudinal lamina; hm, hyomandibular; ih, interhyal; it, intertemporal; ju, jugal; lac, lacrimal; les, lateral extrascapular; lgu, lateral gular; lsc, lateral scute; mes, median extrascapular; mgu, medial gular; mr, median radial; msc, medial scute; mx, maxilla; na, nasal; nppn, notch on parasphenoid; op, opercle; pa, parietal; pas, parasphenoid; pcl, postcleithrum; pcr, procurrent ray; pio, postinfraorbital; pl-a, anterior pit-line; pl-m, median pit-line; pl-p, posterior pit-line; pn, posterior nostril; pop, preopercle; pq, palatoquadrate; pqn, notch of palatoquadrate; pr, principal ray; prl, proximal radial; pt, posttemporal; pv, pelvic plate; qj, quadratojugal; qu, quadrate region of palatoquadrate; r, rostral; sang, supra-angular; sbo, suborbital; sc, scute; scl, supracleithrum; slr, sclerotic ring; sn, supraneural; sop, subopercle; st, supratemporal; vo, vomer.

Measurements CD, depth at base of caudal fin; CL, caudal length; DD, body depth at origin of dorsal fin; HA, length from end of head to origin of anal fin; HD, length from hind of head to origin of dorsal fin; HL, head length; ORB, orbital length; POL, postorbital length of head; SL, standard length; TL, total length (Fig. 2).

3 Systematic paleontology

Subclass Actinopterygii Cope, 1887

Family ? Rhadinichthyidae Romer, 1945

Genus *Pteronisculus* White, 1933

***Pteronisculus changae* sp. nov.**

(Figs. 3–12, 13A, 14A)

Etymology The species name honors Mee-mann Chang for her contributions to paleoichthyological studies in China.

Holotype IVPP V 18994, a nearly complete, laterally compressed skeleton.

Paratype IVPP V 20493, 24340, 25615 and 25618.

Locality and horizon Luoping, Yunnan Province; second (upper) member of Guanling Formation, Pelsonian (~244.2 Ma), Anisian, Middle Triassic (Zhang et al., 2009, 2015).

Diagnosis A large-sized species of *Pteronisculus* distinguished from other species of the genus by the following combination of characters: presence of intertemporal/nasal contact;

presence of medial process at middle portion of intertemporal; medial extrascapular nearly as large as lateral one; postorbital length 60% of head length; suspensorium angle of 35º; opercle three times as deep as subopercle; antopercle half of depth of opercle; presence of 21 supraneurals; and pterygial formula of D53/P15, A44, C71/T83.

4 Description

General morphology and size Similar to other species of *Pteronisculus*, the new species has a blunt snout, an elongate fusiform body, and a heterocercal caudal fin (Figs. 3, 4). The holotype (Fig. 3A) has a total length of 221.0 mm, a standard length of 155.5 mm, and a maximum body depth of 46.5 mm. The largest known specimen has a total length of 295.3 mm, a standard length of 215.0 mm. The measurements of five specimens are presented in Table 1.

Snout The canal-bearing bones in the snout region include a median rostral and a pair

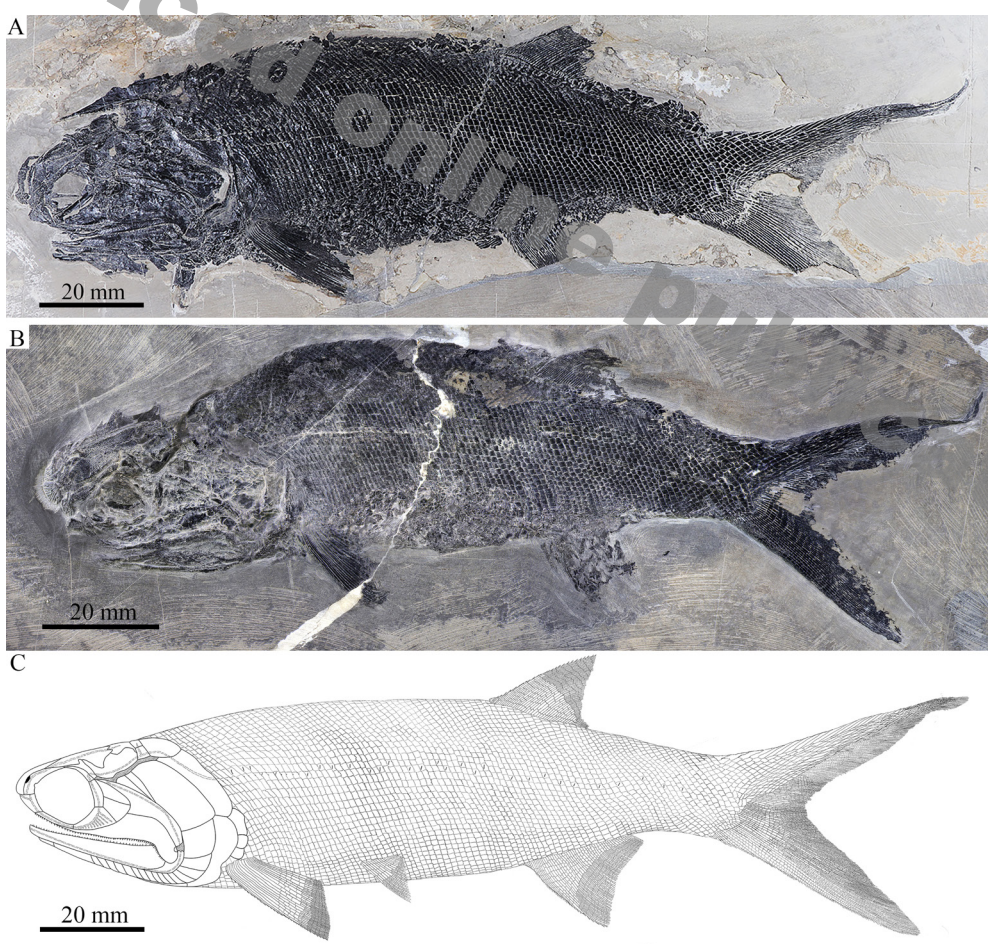

Fig. 3 Specimens and reconstruction of *Pteronisculus changae* sp. nov.
A. IVPP V 18994, holotype; B. IVPP V 20493; C. reconstruction

of nasals and antorbitals (Figs. 5–7, 8A). The median rostral is exposed externally in IVPP V 20493 (Fig. 8A) and internally in V 24340 (Fig. 7). It is large and shield-like and twice as long as it is wide. The lateral margins of the rostral are notched for the anterior nostrils. The length from each notch to the anterior tip is a quarter of the total length of this bone. From this notch, the rostral gradually widens posteriorly, reaches its great width when it contacts the frontals, and then tapers rapidly to a pointed posterior end. The anterior portion of the rostral bends ventrally, having a rounded ventral margin. The external surface of the rostral is strongly ornamented with transverse ridges and tubercles at the posterior portion and longitudinal ridges at the anteroventral portion (Figs. 5, 8A). The ethmoid commissure in the rostral is indicated by an arc of small pores on the external surface of the anteroventral portion (just below the anterior nostril) of this bone (Fig. 5). In addition, there are some pores between both anterior nostrils in the internal surface of the rostral (Fig. 7), which might also indicate the position of the ethmoid commissure in this bone.

Table 1 Measurements of *Pteronisculus changae* sp. nov. from Luoping, Yunnan (mm)

Specimen	ORB	POL	DD	HD	HL	HA	CD	CL	SL	TL
V 18994	9.3	30.2	46.5	56.7	49.1	61.6	21.7	61.2	155.5	221.0
V 24340	10.6	26.7	41.8	49.8	40.1	57.6	19.4	–	138.2	–
V 20493	7.0	23.4	34.0	38.8	38.2	43.5	15.8	44.3	118.7	163.3
V 25615	13.2	31.7	51.5	57.7	52.5	60.1	23.4	65.5	156.0	221.5
V 25618	17.4	34.1	58.4	76.8	64.1	83.1	30.0	80.3	215.0	295.3

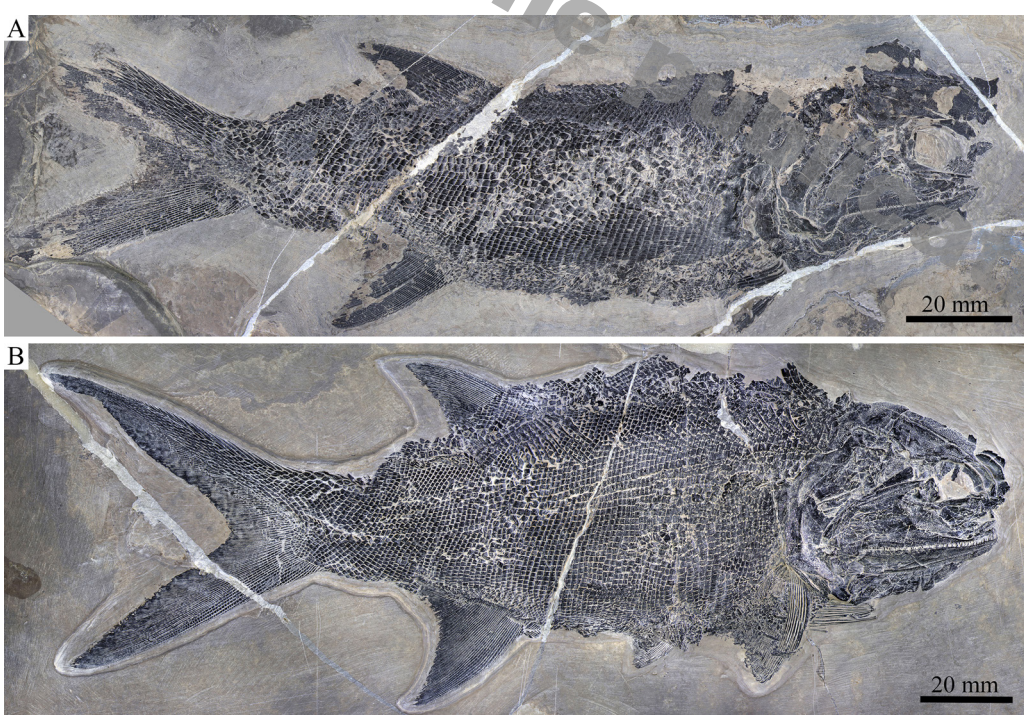

Fig. 4 Two specimens of *Pteronisculus changae* sp. nov.
A. IVPP V 24340; B. IVPP V 25615

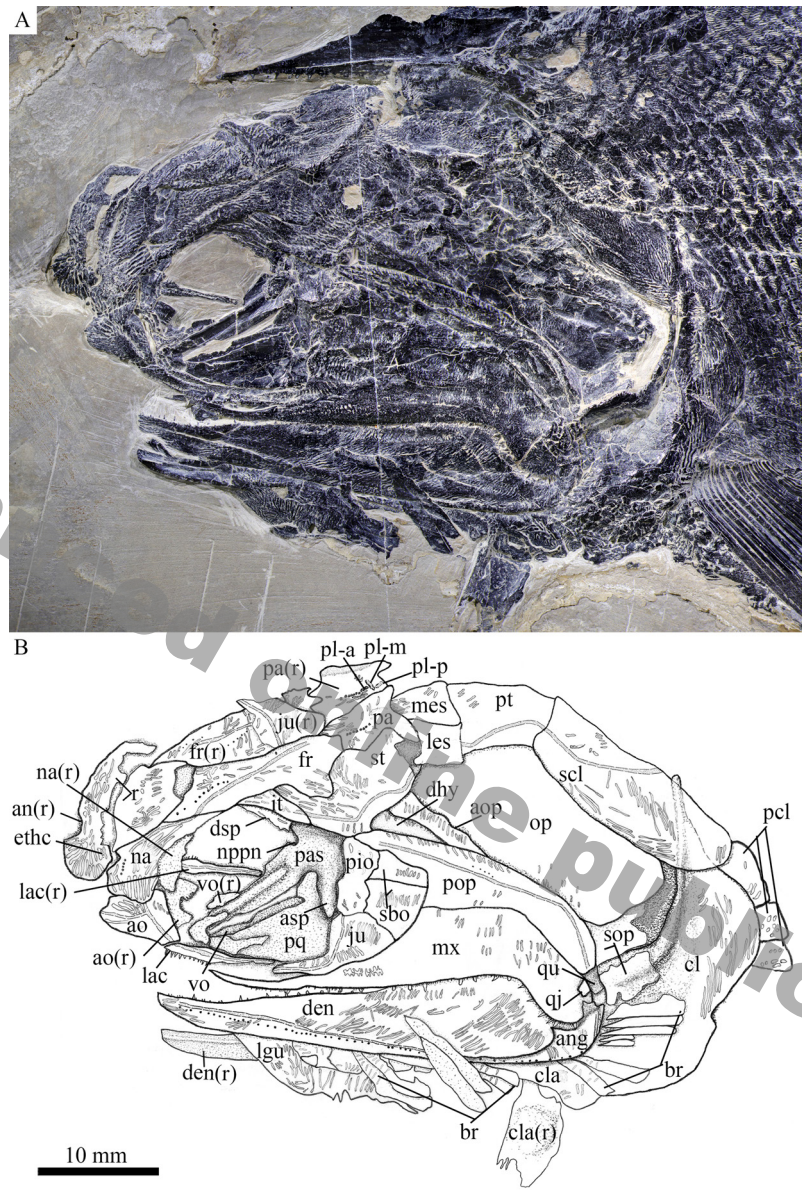

Fig. 5 Photograph (A) and line-drawing (B) of skull and pectoral girdle of *Pteronisculus changae* sp. nov., IVPP V 18994 (holotype)

The nasals are narrow and elongate, slightly shorter than the rostral, tapering posteriorly. Each nasal contacts the rostral and frontal medially, and the dermosphenotic and intertemporal posteriorly (Figs. 5, 7, 8A). The lateral margin of the nasal is slightly notched for the posterior nostril, and defines the anterodorsal margin of the orbit. A semicircular notch for the anterior nostril is present in the medial margin of the nasal, corresponding to the notch in the lateral margin of the rostral. Indicated by several small pores, the nasal bears an anterior portion of the supraorbital sensory canal that curves ventrally from the frontal and terminates just below the level of the anterior nostril. The external surface of the nasal is ornamented with a series of longitudinal ridges (Figs. 5, 8A).

Fig. 6 Photograph (A) and line-drawing (B) of skull and pectoral girdle of *Pteronisculus changae* sp. nov., IVPP V 25615

The antorbital is nearly trapezoidal, contacting the nasal dorsally, the rostral anteromedially and the lacrimal posteriorly (Figs. 5, 7, 8A). The ventral margin of the antorbital forms a short anterior length of the oral margin, and its posterodorsal margin contributes to the composition of the anterior orbital margin. The infraorbital canal and ethmoid commissure meet on this bone and form a tripartite junction. The surface of the

antorbital is ornamented with horizontal ridges.

Skull roof The skull roof is comprised of a pair of frontals, parietals, intertemporals, supratemporals and two pairs of extrascapulars. These elements are ornamented with dense ridges and tubercles.

The frontals are roughly trapezoidal, 2.5 times as long as the parietal (Fig. 6). The majority of the frontal contacts its counterpart medially in a meandrous suture, except a short anterior portion which tapers anterolaterally to a point and flanks the posterior portion of the rostral (Figs. 6, 8A). There is no pineal foramen between the frontals. The supraorbital sensory canal extends longitudinally through each frontal and enters the parietal posteriorly. The sensory pores are located lateral to the sensory canal at the anterior half portion of the frontal and medial to the canal at the posterior half portion of this bone.

The parietals are nearly rectangular, slightly longer than they are broad, with a short posterolateral extension. Each parietal contacts the frontal anteriorly along a zigzag suture and the supratemporal laterally along a curved suture (Fig. 6). The medial and posterior margins of the parietal are nearly straight. Three pit-lines are present in the parietal; the anterior pit-line is continuous with the supraorbital sensory canal, the middle one extends anterolaterally for a relatively short length, and the posterior one extends posterolaterally and terminates near the posterior margin of this bone (Figs. 5, 6).

The intertemporals are triradiate, having pointed anterior and posterior tips and a medially directed process at the middle portion of this bone (Fig. 6). Each intertemporal is about half of the frontal length, contacting the anterior portion of the frontal medially, the anterior portion of the supratemporal posteromedially, and the dermosphenotic anterolaterally. Anteriorly, the intertemporal tapers to a point and terminates slightly anterior to the junction of the frontal and the nasal.

The supratemporals are large and irregular, twice the length of the intertemporal or parietal. The anterior part of the supratemporal tapers anteromedially and inserts between the frontal and intertemporal. The medial suture with the frontal is rather concave, and the anterolateral suture with the intertemporal is convex. The later margin of the supratemporal is notched at its middle portion (Figs. 5–7), similar to other species of *Pteronisculus* (Nielsen, 1942; Xu et al., 2014b). The supratemporal sensory canal extends longitudinally through the lateral portions of the intertemporal and supratemporal, and posteriorly enters the lateral extrascapular.

Two trapezoidal extrascapulars are present at each side of the skull (Figs. 5, 6). The lateral extrascapular is nearly equal to the medial one in width. The median extrascapular extends medially to the midline of the skull. The supratemporal commissure runs traversely through the middle portions of both extrascapulars.

Cheek The cheek region includes three infraorbitals (lacrimal, jugal and postinfraorbital), two suborbitals, a quadratojugal, a preopercle, a dermohyal and an antopercle.

The lacrimal is elongate and one third as long as the maxilla. The anterior half of the

ventral margin of the lacrimal forms a part of the oral margin and bears conical teeth (Fig. 5), characteristic of *Pteronisculus* (Xu et al., 2014b). The jugal is relatively large and pentagonal, defining the posteroventral margin of the orbit. The lacrimal passes the infraorbital sensory canal from the antorbital to jugal, in which the canal has about ten rami.

The postinfraorbital is small and narrow, contacting the jugal ventrally, the dermosphenotic dorsally, and the suborbitals posteriorly (Fig. 5).

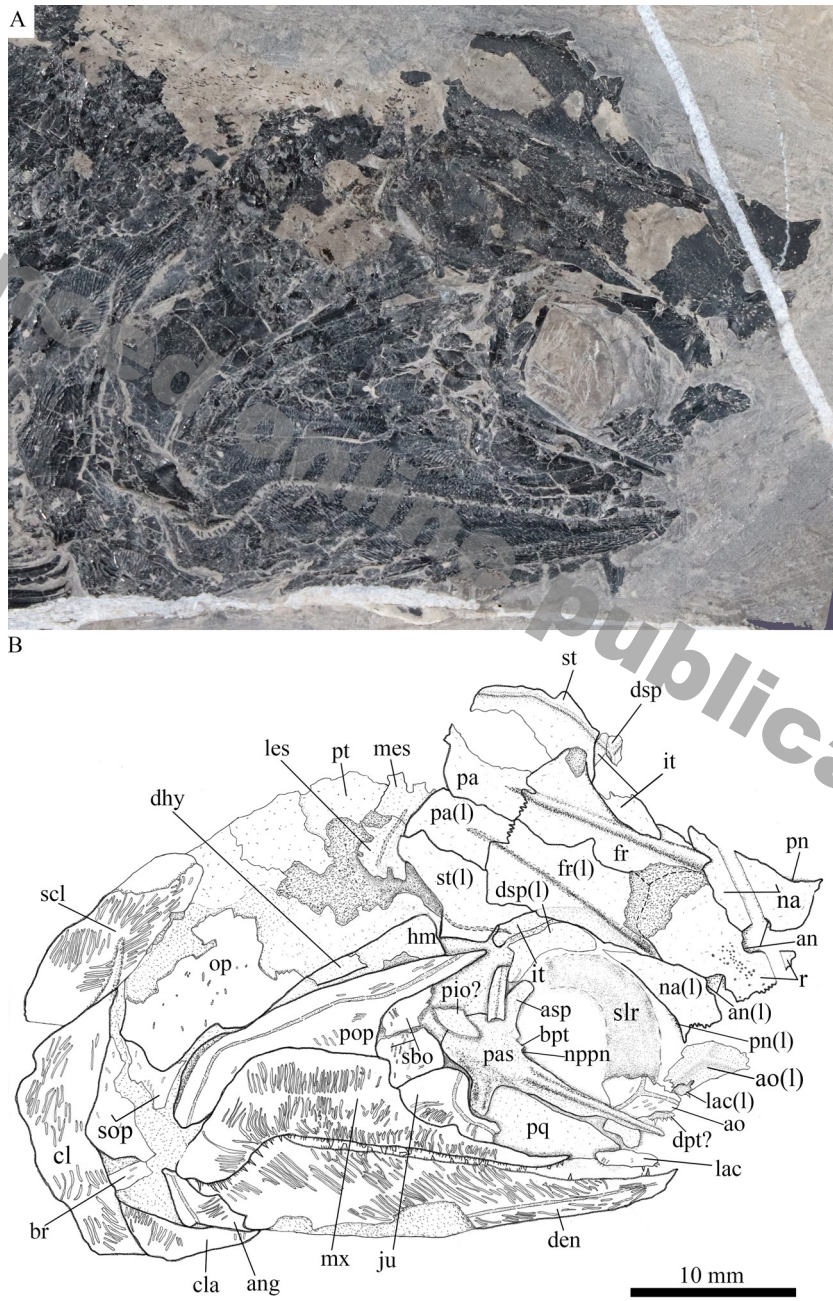

Fig. 7 Photograph (A) and line-drawing (B) of skull and pectoral girdle of *Pteronisculus changae* sp. nov., IVPP V 24340

The dermosphenotic is exposed laterally in IVPP V 18994 and V 25615 (Figs. 5, 6), and medially in V 24340 (Fig. 7). This bone is roughly triangular, contacting the intertemporal posterodorsally and the nasal anteriorly.

There are two suborbitals between the third infraorbital and the preopercle, including a trapezoidal ventral one and a triangular dorsal one (Fig. 5). Both are ornamented by some short striae and tubercles.

The quadratojugal, discernable in V 18994 and V 25615 (Figs. 5, 6), is small and subcircular, contacting the quadrate portion of the palatoquadrate laterally and the maxilla anteriorly.

The preopercle is hatchet-shaped, consisted of a triangular anterodorsal limb and a narrow posteroventral stem (Figs. 5–7). It tapers to a point anterodorsally and nearly reaches the anteroventral tip of the supratemporal. The preopercular canal extends through the preopercle near the posterior margin of this bone, having a series of small pores located posterodorsal to the canal (Figs. 5, 6).

The dermohyal is small, narrow and triangular, tapering ventrally (Fig. 6). It is wedged between the preopercle and antopercle, ornamented with several striae on its external surface. Medially, it is bound to the lateral surface of the hyomandibula.

In addition, there is a narrow, deep and triangular bone inserting between the dermohyal and opercle (Fig. 5). This bone is labeled as the antopercle, following Nielsen (1942).

Operculo-gular series The opercle is large, nearly rhomboid and anteriorly inclined, and the subopercle is equilateral with half of the depth of the opercle (Fig. 5). The branchiostegal rays are slender and lamellate. Eight branchiostegal rays are preserved below the dentary in V 25615 (Fig. 6) and seven are posterior to the angular in V 18994 (Fig. 5). Thus, a complete series of 15 branchiostegal rays is reconstructed at each side of the skull (Fig. 3C).

Anterior to the first branchiostegal ray, a right lateral gular is exposed in V 25615 (Fig. 6). It is relatively broad and large, being about one-fourth of the length of the lower jaw. The median gular is not exposed.

Parasphenoid, vomers and palatoquadrate Most of the parasphenoid, vomers and palatoquadrate are discernable through the orbit. The parasphenoid is elongate, slightly longer than the frontal (Figs. 6, 7, 8A). The median keel of this bone tapers anteriorly, having a narrow anterior tip and a rounded posterior margin. Two lateral processes are present on either side of the posterior portion of the parasphenoid, including a short basipterygoid process and a deep ascending process (Fig. 7, 8A). Dense small conical teeth are present on the ventral margin of the parasphenoid anterior to the basipterygoid process (Fig. 8A). There is no buccohypophyseal opening nor are there other pores discernable in this bone, which is similar to other species of *Pteronisculus* (Nielsen, 1942). Anterior to the base of each basipterygoid process is the small notch for the pseudobranchial efferent artery (Figs. 7, 8A).

The paired vomers are small and slender, bearing small teeth on its ventral margin (Fig.

8A). The teeth are conical and similar in size to those on the parasphenoid.

The exposed anterodorsal portion of the palatoquadrate is nearly triangular and has a distinct notch on the dorsal margin of its metapterygoid portion for articulating with the basipterygoid process (Figs. 7, 8A). Additionally, a small quadrate portion of the palatoquadrate is exposed, articulating with the lower jaw ventrally (Fig. 6).

Hyomandibula and interhyal The hyomandibula is situated at an oblique angle of 35°, bearing a short and strong opercular process at the posterior margin of this bone (Fig. 6). Most of this bone is laterally covered by the preopercle and dermohyal, and its complete shape remains unknown.

An interhyal is preserved ventral to the hyomandibula and posterior to the quadrate portion of the palatoquadrate (Fig. 6). It is small and nearly cylindrical.

Upper jaw No premaxillae are discernable, and they are probably lost or fused with lacrimal (Xu et al., 2014b).

The maxilla has a dorsoventrally short and elongate suborbital ramus and a deeper posterodorsal blade with a pronounced posteroventral process laterally covering the posterior portion of the lower jaw (Figs. 5–7). It contacts the preopercle along its convex posterodorsal margin. The outer surface of the maxilla is ornamented with some short ridges. In medial view,

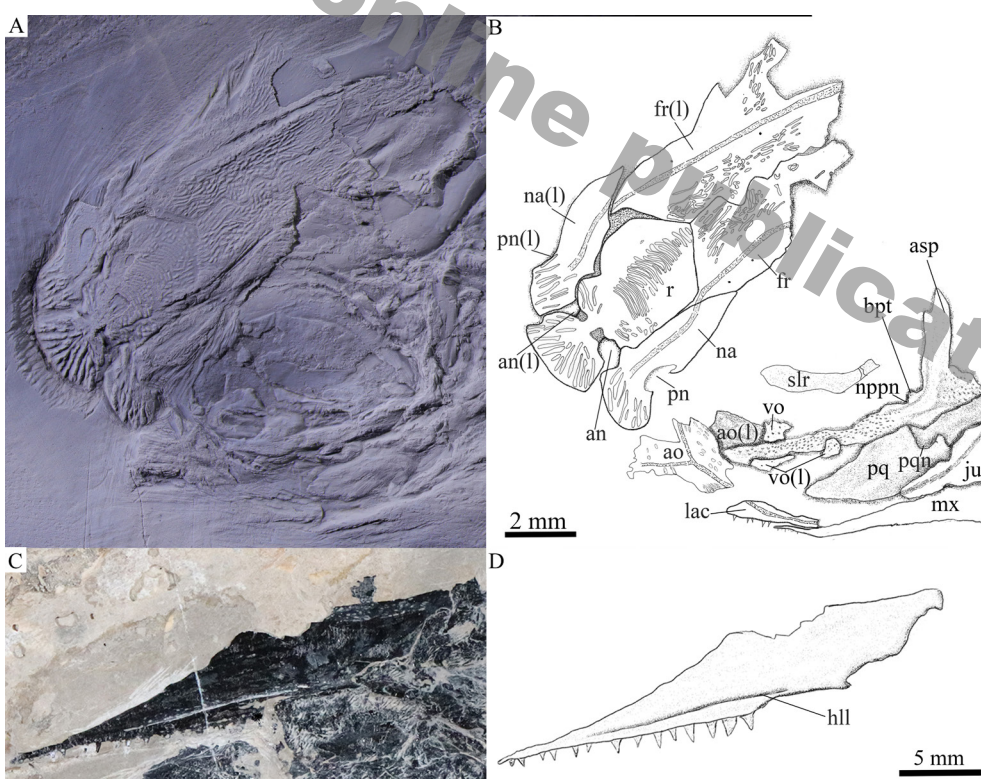

Fig. 8 Anterior portion of skull and cheek region of *Pteronisculus changae* sp. nov.
A. anterior potion of skull, IVPP V 20493, dusted with ammonium chloride; B. line-drawing of A; C. maxilla in medial view, IVPP V 18994; D. line-drawing of C

the maxilla has a horizontal longitudinal lamina parallel to its ventral margin (Fig. 8C), as in other species of *Pteronisculus* (Nielsen, 1942). The dentition consists of numerous minute teeth on the outer edge and an inner row of larger conical laniary teeth (Figs. 5–7).

Lower jaw The dentary is large and elongate with a slightly concave dorsal (oral) margin, a convex ventral margin and a curved posterior margin. The dentition on the oral margin of this bone consists of longer teeth interspersed with shorter and smaller denticles.

The angular is slender and wedge-shaped, tapering anteroventrally. The supra-angular is small and not fully exposed, laterally covered by the posteroventral process of the maxilla (Fig. 6). The dentary and angular are ornamented by prominent ganoine ridges, and the supra-angular is smooth. The mandibular sensory canal extends the whole length of both the dentary and angular, with a series of small openings located ventral to the canal. (Figs. 5, 6).

The ossified articular region of the Meckelian cartilage is partly exposed laterally, having a rounded fossa that articulates with the lateral condyle of the quadrate portion of the palatoquadrate (Fig. 6).

The coronoids and prearticular are unknown because the medial surface of the lower jaw is not exposed.

Girdles and paired fins The posttemporals are fan-shaped, contacting the extrascapulars anteriorly and the supracleithrum posteroventrally (Figs. 5, 6). The supracleithrum is deep and relatively narrow with convex ventral and posterior margins. The lateral line sensory canal pierces the lateral portion of the posttemporal and extends posteroventrally into the supracleithrum.

The cleithrum is large and curved, having a concave anterior margin and a curved posterior margin. The dorsal tip is pointed, partly covered by the supracleithrum (Fig. 5). The clavicle is small and triangular, contacting the cleithrum posterodorsally. The exposed surfaces of the cleithrum and clavicle are ornamented with ganoine ridges.

The pectoral fins are large and relatively long, inserting low on the body. Each pectoral fin has about 20 distally segmented and branched rays, preceded by a basal fulcrum and a series of fringing fulcra (Fig. 9A).

The pelvic plate is elongate with a triangular posterior base and a slender anterior process (Fig. 9C).

The pelvic fins are relatively small and are located at the 15th vertical scale row. Each includes about 15 distally segmented and branched rays. Fringing fulcra are also present on the leading margin of the fin (Fig. 9B).

Median fins The triangular dorsal fin originates above the 53rd vertical scale row, and its base occupies the length of 14 vertical scale rows. It is composed of 31 principal fin rays, preceded by nine procurrent rays and two small basal fulcra (Fig. 10D). All rays are segmented through their length. The first principal ray is unbranched and five-sixths as long as the second principal ray. The latter branches once distally, being the longest ray of the dorsal fin. Other rays branch twice and gradually decrease in length posteriorly. A series of small fringing fulcra

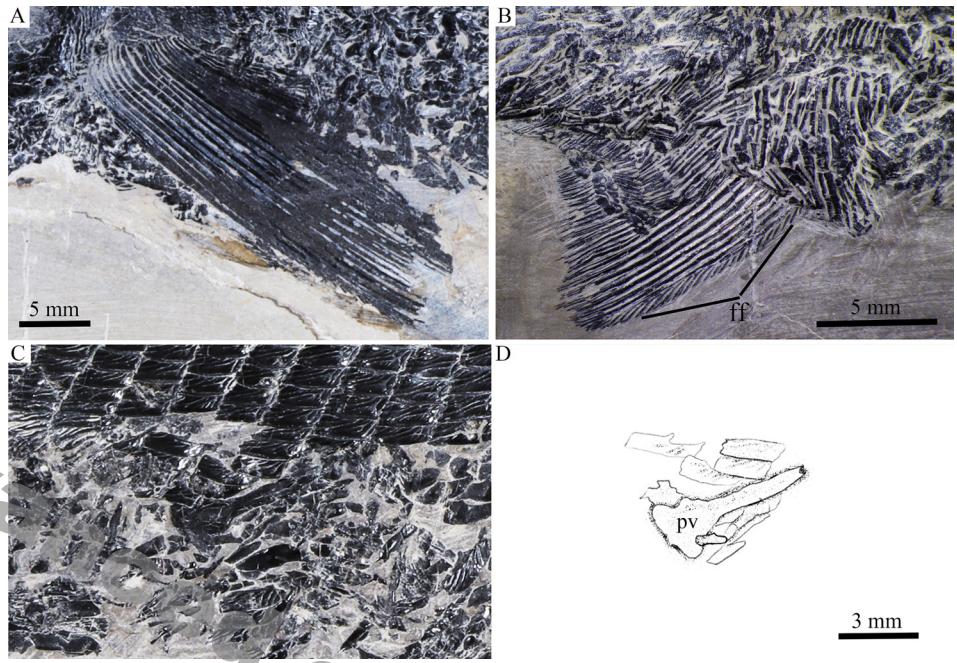

Fig. 9 Paired fins of *Pteronisculus changae* sp. nov.
A. left pectoral fin, IVPP V 18994; B. right pelvic fin, V 25615;
C. right pelvic plate, V 24340; D. line-drawing of C

is associated with the anterior margins of all procurrent rays, and the first and second principal rays (Fig. 10D). A series of middle and proximal radials are discernable in the pterygiophores that support the dorsal fin; the distal radials, probably not ossified or unexposed, remain unknown. There are 11 middle radials present; they are rod-like or hour-glass shaped, slightly expanding at both ends (Fig. 12). Among them, the anterior two are slightly shorter than the third, which is the longest; and other radials gradually become shorter posteriorly. There are 11 proximal radials, which are 2.7–3.0 times as long as the middle radials. They are rod-like with a slightly expanded distal portion. The first radial is the longest and strongest, and the remaining gradually become shorter posteriorly.

The anal fin originates below the 44th vertical scale row, and its base extends the length of about 20 vertical scale rows. It is also triangular and one-third larger than the dorsal fin. The anal fin is composed of 41 principal fin rays, which are preceded by nine procurrent rays and a basal fulcrum (Fig. 10C). The second and third principal rays branch once; the latter is the longest ray of the anal fin. The remaining rays branch up to three times and gradually decease in length posteriorly. Similar to those in the dorsal fin, a series of fringing fulcra are associated with the anterior margins of all procurrent rays and the first and second principal rays.

The caudal fin is heterocercal with a deeply forked profile. The dorsal lobe, which is slightly longer than the ventral one, has a small epichordal lobe at its distal tip (Fig. 10B). About 70 segmented principal rays are present with 20 in the dorsal lobe (Fig. 10A). Additionally, there are nine unbranched procurrent rays preceding the ventral most principal

ray. The middle principal rays are distally branched up to five times. About 20 epaxial basal fulcra are present; they are elongate and taper posteriorly. The hypaxial basal fulcra are relatively short, two or three in number. Small leaf-like fringing fulcra are present in both lobes of the caudal fin (Fig. 10A).

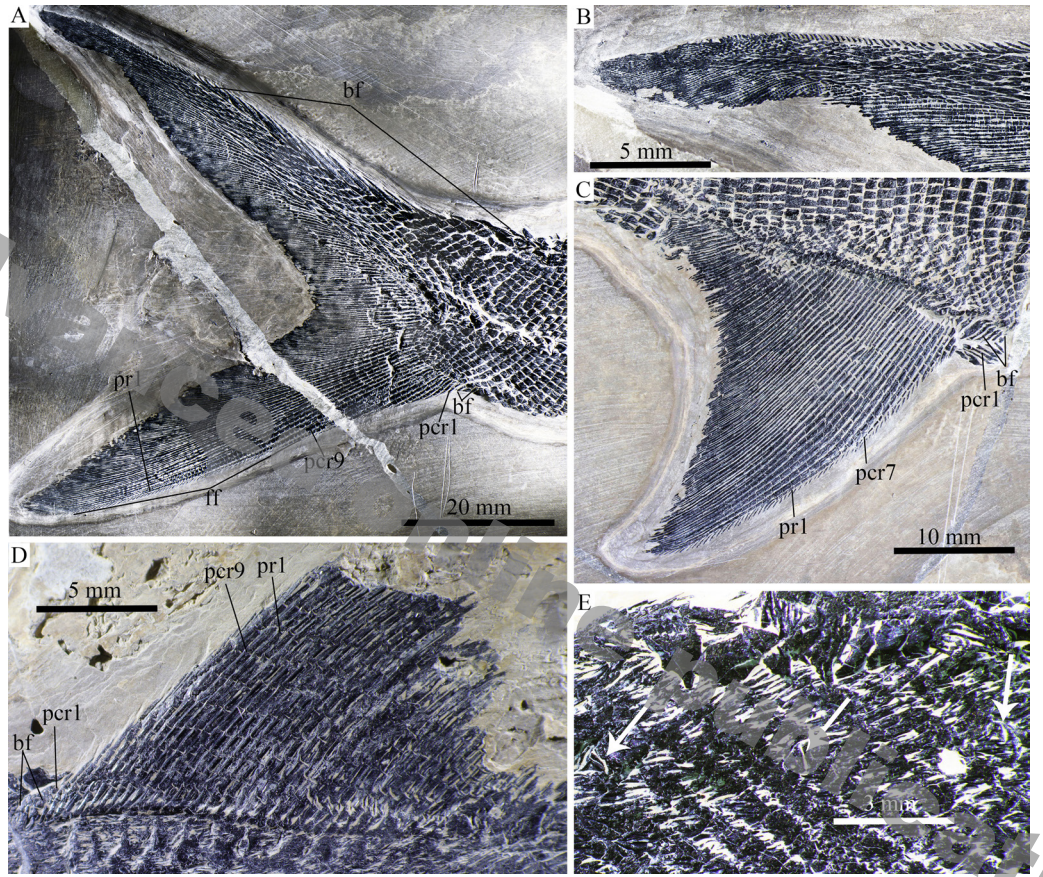

Fig. 10 Fins and scales of *Pteronisculus changae* sp. nov.
A. caudal fin, IVPP V 25615; B. close up of epichordal lobe of caudal fin in A; C. anal fin, V 25615; D. dorsal fin, V 18994; E. pit organs in pre-dorsal region, V 18994

Squamation The scales are rhomboid with serrated posterior margins. They are arranged in 83 transverse rows of scales between the posterior margin of the supracleithrum and the caudal inversion. The scales in the anterior flank region are slightly deeper than they are long, and they gradually become shorter and smaller dorsally and ventrally. In the middle flank region at each side of body, 15 horizontal rows of scale lie above the main lateral line, and 17 below (Figs. 3A, C). The trajectory of the main lateral line is indicated by a series of small pores in the scales of the anterior flank region. Additionally, every two to five lateral line scales have a dorsoventrally extended slit (Figs. 11D–F), which probably represents the individual pit organ that is separate and independent from the lateral line canal (Schultze, 1966). Besides those in the lateral line scales, some of anterior pit organs are also present in the

adjacent row of scales above the lateral line (Fig. 11F). Moreover, an accessory dorsal lateral line lies close to the dorsal margin of the body, indicated by several slits in the predorsal region (Fig. 10E). There are a pair of enlarged lateral scutes anterior to the anal fin (Fig. 11A) and three median scutes preceding the basal fulcra at the ventral lobe of the caudal fin (Fig. 11B). Peg-and-socket articulations are exposed between some scales in the anterior flank region (Fig. 11C). The scales are ornamented with fine and diagonally directed ridges (Figs. 11C–E).

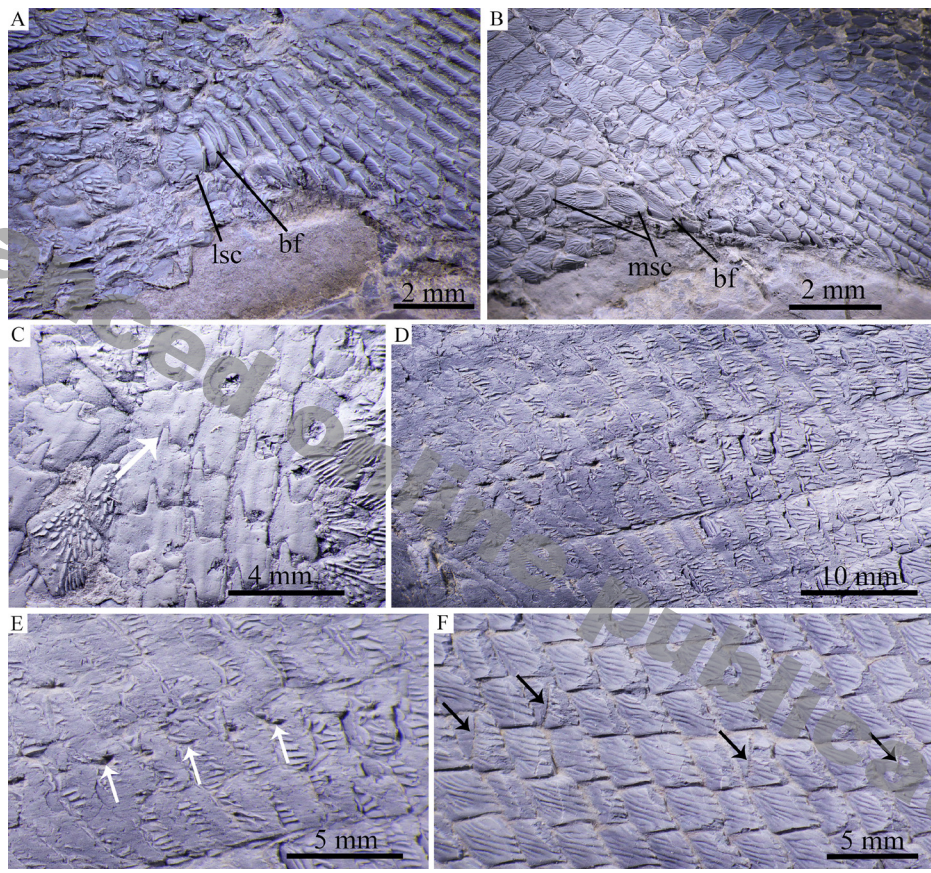

Fig. 11 Scales of *Pteronisculus changae* sp. nov., IVPP V 25618, dusted with ammonium chloride
A. scutes anterior to the anal fin; B. scutes anterior to the ventral lobe of the caudal fin;
C. peg-socket articulation between scales; D. lateral line scales;
E. scales with white arrows indicating sensory pores; F. scales with black arrows indicating pit organs

Axial skeleton Only the supraneurals are exposed; other elements of the axial skeleton remain unknown because of the coverage of the scales (Fig. 12). Twenty supraneurals are counted posterior to the supracleithrum and below the anterior four middle radials of dorsal fin. They are slender, slightly curved posteroventrally and posteriorly inclined. Additionally, there is an obvious gap posterior to the seventh supraneural, which indicates a missing supraneural. Thus, the whole series would include 21 supraneurals; 17 of those anterior to the dorsal fin and four below the dorsal fin pterygiophores.

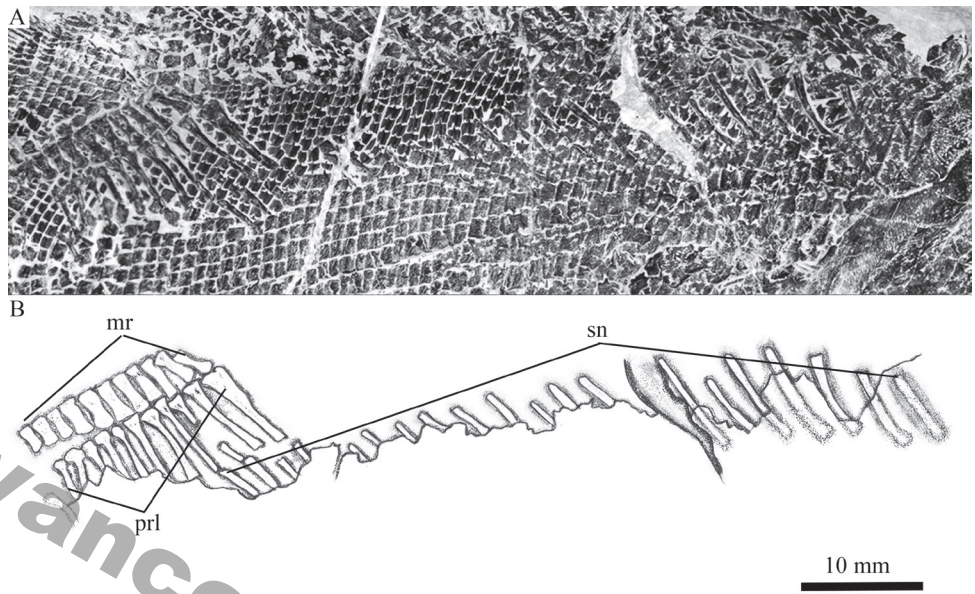

Fig. 12 Photograph (A) and line-drawing (B) of supraneural bones and pterygiophores supporting the dorsal fin of *Pteronisculus changae* sp. nov., IVPP V 25615

5 Discussion

5.1 Character comparisons

Pteronisculus changae sp. nov. is easily distinguished from *P. nielseni* also from the Luoping Biota and other older species of this genus outside of China in the following aspects:

(1) A medial process at the middle portion of the intertemporal. *P. changae* has a triradiate intertemporal with a medial process at the middle portion of this bone. By contrast, the intertemporal in other species of the genus is elongate or triangular and lacks a median process (Fig. 13).

(2) A postorbital skull length to skull length ratio of 60%. In this ratio, *P. changae* is slightly longer than *P. nielseni* (57%) but shorter than other species of the genus (e.g., 64% in *P. cicatrosus*, 70% in *P. stensioi*, and 72% in *P. magnus*).

(3) Presence of an antopercle. There is an antopercle between the dermohyal and opercle in *P. changae* (Fig. 13). This bone is otherwise present in *P. stensioi*, *P. cicatrosus*, *P. magnus* and some other early actinopterygians, but it is absent in *P. nielseni*.

(4) A relatively broad and large medial extrascapular. The medial extrascapular is nearly as broad as the lateral extrascapular in *P. changae*, but the former is generally narrower and smaller than the latter in other species of this genus (Fig. 14).

(5) A suspensorium angle of 35º. In the suspensorium angle (Fig. 15), *P. changae* shows an intermediate state between *P. nielseni* (40°) and other species of the genus surveyed herein (about 30°).

(6) Presence of 21 supraneurals. *P. changae* has the largest number of supraneurals in this genus (Fig. 12). However, *P. magnus* and *P. gunnari* generally have about 15–18 supraneurals (Nielson, 1942).

(7) A large number of lateral line scales. *P. changae* has 83 lateral line scales, representing the largest number known in this genus. In comparison, other species of the genus generally have 55–65 lateral line scales (55–59 in *P. arctica*, 63 in *P. stensioi*, ~65 in *P. aldingeri*, and 60–61 in *P. nielseni*; for comparisons of pterygial formula in selected species of *Pteronisculus*, see on-line supplementary martial).

(8) Deep and numerous pit organs in scales. The pit organs associated with the lateral line system are only slightly shorter than the scales in *P. changae* (Fig. 11D). However, the

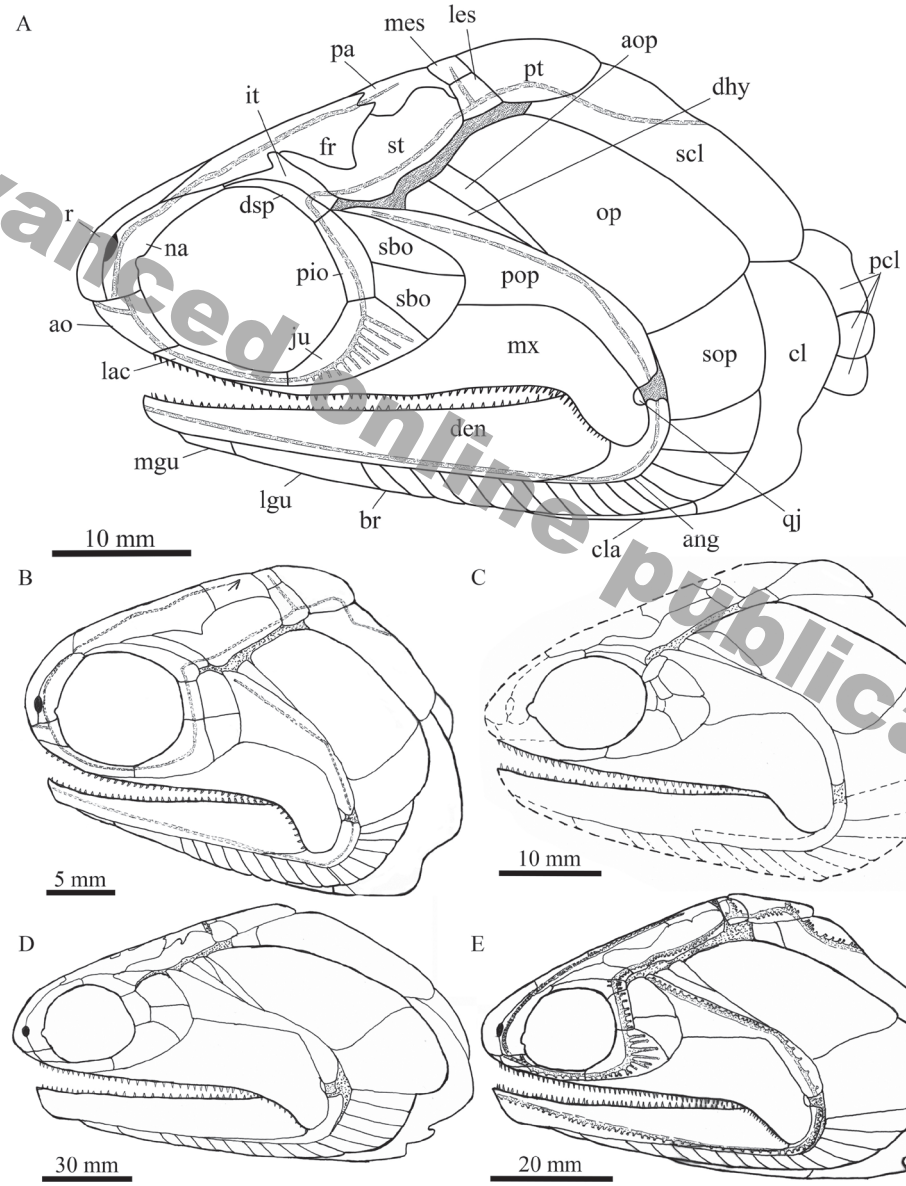

Fig. 13 Reconstructions of skulls and pectoral girdles of selected species of *Pteronisculus* in lateral view A. *Pteronisculus changae* sp. nov.; B. *P. nielseni* (from Xu et al., 2014b); C. *P. cicatrosus* (from Lehman, 1952). D. *P. magnus* (from Nielsen, 1942); E. *P. stensioi* (from Nielsen, 1942)

pit organs are dorsoventrally much shorter (i.e., no more than one third of the scale depth) in *P. nielseni*. In addition, *P. changae* has a greater number of pit organs (26 in IVPP V 18994), which are distributed not only in the lateral line scales but also in the adjacent row of scales above the lateral line. By contrast, the pit organs in *P. nielseni* are fewer in number (16 in V 25661), mainly confined in the lateral line scales. The pit organs were not identified in the

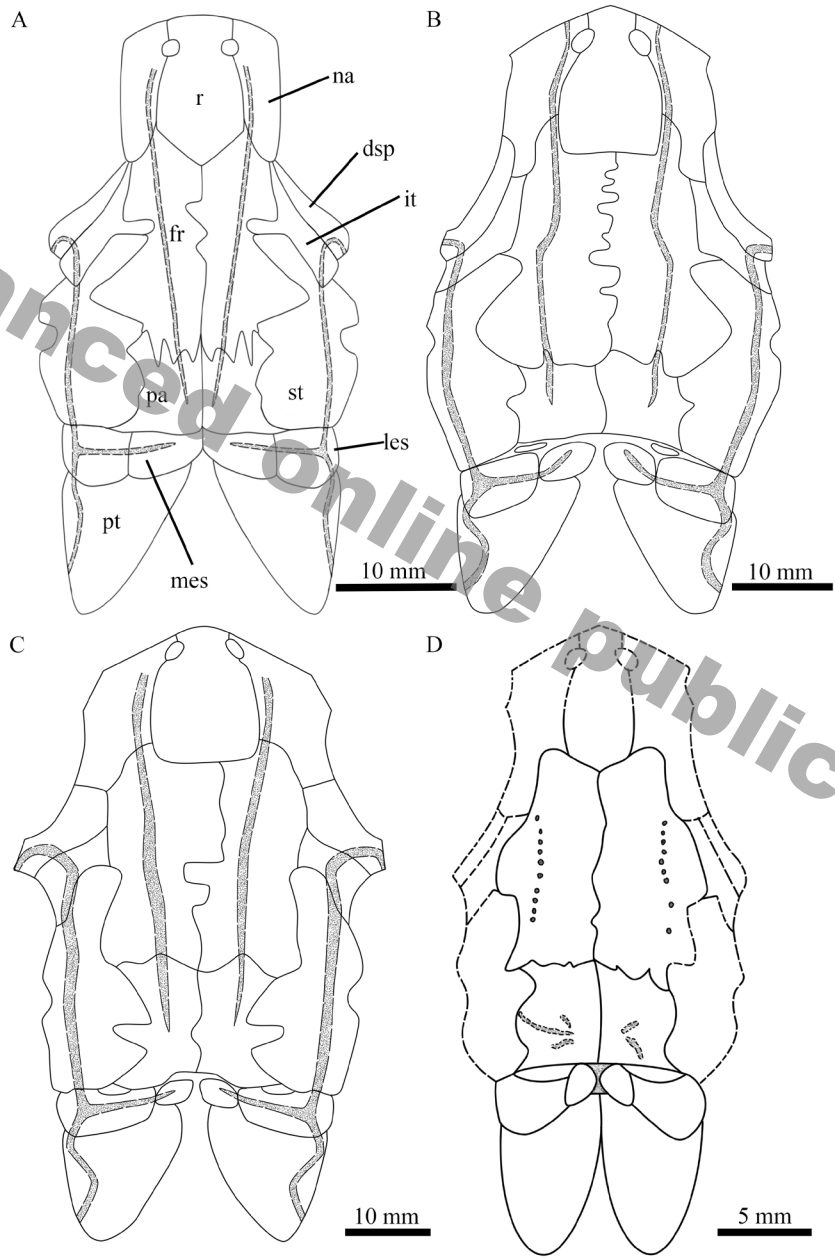

Fig. 14 Reconstructions of skulls of selected species of *Pteronisculus* in dorsal view
A. *Pteronisculus changae* sp. nov.; B. *P. stensioi* (from Nielsen, 1942); C. *P. magnus* (from Nielsen, 1942); D. *P. cicatrosus* (from Lehman, 1952)

previous description of the genus outside of China, and further studies are needed to clarify their presence in Early Triassic species.

5.2 Phylogenetic analysis

Phylogenetic analysis recovered 12 most parsimonious trees (tree length = 996 steps, consistency index = 0.3002, retention index = 0.6715). The strict consensus cladogram is shown in Fig. 16. *Pteronisculus* is recovered as a sister taxon of the Carboniferous rhadinichthyid *Cyranorhis* at the Actinopterygii stem. The Cladistia (including Scanilepiformes) forms the sister group of the Actinopteri (Chondrostei plus Neopterygii) within the Actinopterygii crown, consistent with other recent phylogenies (Giles et al., 2017; Wilson et al., 2018). The Birgeriiformes and Saurichthyiformes are nested at the Chondrostei stem, in accordance with Gardiner et al. (2005) and Xu and Gao (2011); by contrast, both clades are recovered at the Actinopterygii stem by other recent analyses (Giles et al., 2017; Argyriou et al., 2018). Additionally, some deep-bodied taxa (*Discoserra*, *Ebenaqua* and *Bobasatrania*) are also recovered at the Chondrostei stem rather than the Neopterygii stem (in contrast to Hurley et al., 2007; Xu et al., 2014a; Giles et al., 2017; Argyriou et al., 2018).

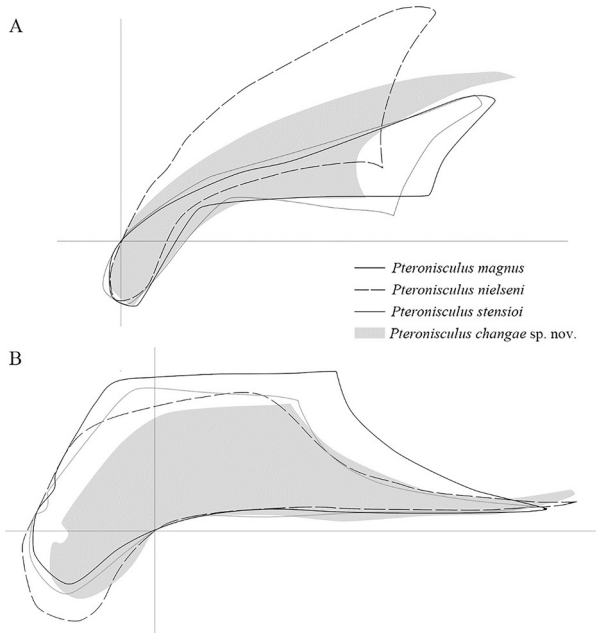

Fig. 15 Comparisons of preopercles (A) and maxillae (B) in different species of *Pteronisculus*
Not to scale

The genus *Cheirolepis* (including three species) is recovered at the base of the Actinopterygii. *Raynerius* is more derived than *Cheirolepis* due to the presence of three apomorphies shared with other actinopterygians: 1) contribution of nasals to orbital margins, 2) presence of acrodin caps on teeth, and 3) presence of a narrow interorbital septum. In Devonian actinopterygians, a monophyletic group involves *Howqualepis*, *Mimipiscis* (= *Mimia*), *Osorioichthys* and *Moythomasia*; the sister group relationships between *Osorioichthys* and *Moythomasia* are newly recognized, supported by four character states: 1) the presence of two pairs of extrascapulars, 2) extrascapulars not reaching the lateral edge of the skull roof (reversal in *M. nitida*), 3) a mandibular canal arching dorsally in the anterior half of the lower jaw (reversal in *M. durgaringa*), and 4) the dorsal-most branchiostegal ray deeper than the adjacent one (independently evolved in many other actinopterygians such as *Boreosomus*, *Mesopoma*, *Kalops*, *Teffichthys*, *Caturus* and *Atractosteus*). *Kentuckia* is the most derived of Devonian actinopterygians, as has generally been found in other phylogenies (Swartz, 2009;

Choo, 2011; Xu et al., 2014a). Additionally, the Carboniferous Eurynotiformes (represented by *Amphicentrum*, *Fouldenia* and *Styracopterus*) is well supported as a monophyletic group that consists of the sister group of *Melanecta*, *Woodichthys* plus other more derived actinopterygians.

Further up the tree, the *Cyranorhis*-*Pteronisculus* clade is recovered sister to a monophyletic group involving *Boreosomus*, *Mesopoma*, *Cosmoptychius*, *Beagiascus*, *Aesopichthys* and *Kalops*, supported by four derived features: 1) presence of an anterior junction of supraorbital and infraorbital canals between external nares (independently acquired in *Mimipiscis*, *Osorioichthys*, *Moythomasia*, *Kentuckia*, basal chondrosteans and holosteans), 2) presence of an hourglass-shaped anterior ceratohyal (independently evolved in *Ebenaqua* plus more derived chondrosteans and most neopterygians), 3) presence of jointed radials supporting pectoral fins (independently evolved in *Cheirolepis canadensis*), and 4) presence of an epichordal lobe of the caudal fin (independently acquired in *Cheirolepis*, *Howqualepis*, *Fouldenia* and *Styracopterus*). The sister taxon relationships between *Pteronisculus* and *Cyranorhis* are supported by six derived characters states: 1) presence of a lacrimal contributing to the oral margin (probably also present in *Turseodus*; Schaeffer, 1967; Romano et al., 2019), 2) absence of distinct premaxillae (independently evolved in *Styracopterus* and most chondrosteans), 3) presence of an antorbital bone (independently acquired in *Cosmoptychius*, *Beagiascus*, *Aesopichthys*, *Kalops*, *Birgeria* and neopterygians), 4) presence of two suborbital bones (three in *P. cicatrosus*), 5) presence of an opercle significantly higher than the subopercle, and 6) presence of a presupracleithrum (last two features independently evolved multiple times in other actinopterygians).

The monophyly of *Pteronisculus* is supported by three synapomorphies: 1) presence of teeth on the lacrimal (uniquely derived), 2) presence of a supratemporal ending at the level of the posterior margin of the parietal (reversal in *P. stensioi*, absence in *Mesopoma*, *Cosmoptychius*, *Beagiascus*, *Kalops* and most crown actinopterygians), and 3) presence of three infraorbitals (independently evolved in *Boreosomus* and *Australosomus*). Within *Pteronisculus*, *P. nielseni* is located at the basal position as it possesses the above synapomorphies but lacks a uniquely derived feature shared by all other species of the genus, which is the presence of an antopercle inserting between the dermohyal and opercle. *P. changae* sp. nov., *P. cicatrosus* and *P. stensioi* are more derived than *P. magnus* in possessing the intertemporal/nasal contact and lacking the dermosphenotic/frontal contact. However, the interrelationships between these three species are unresolved, and they form a polytomy within the genus.

Within the actinopterygian crown, the sister group relationships between Cladistia (scanilepiforms plus polypterids) and Actinopteri (Chondrostei plus Neopterygii) are supported (Giles et al., 2017). Notably, *Birgeria* is recovered at the base of the Chondrostei, in accordance with some other analyses (Gardiner et al., 2005; Xu et al., 2014a; but see Giles et al., 2017; Argyriou et al., 2018). Saurichthyiformes is more derived than *Birgeria*,

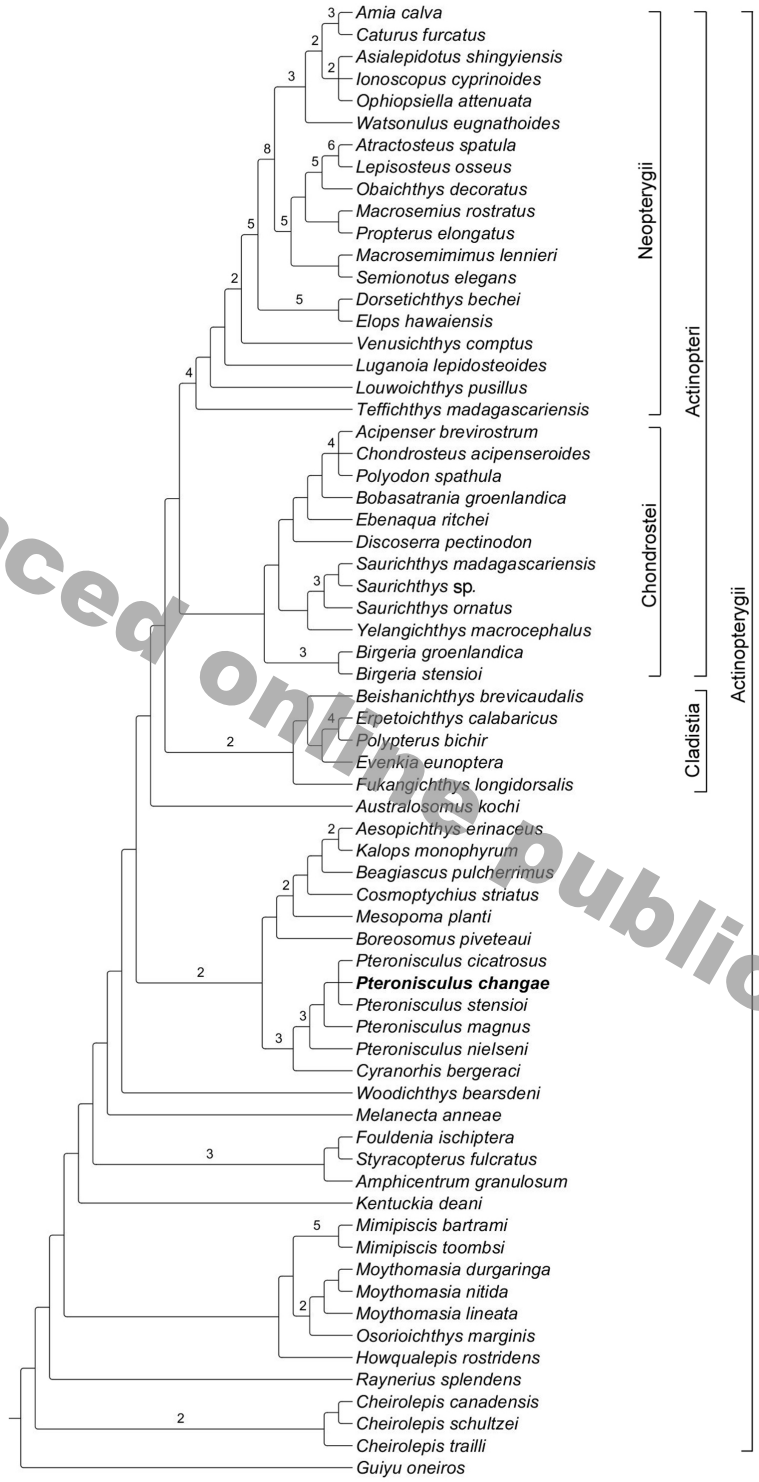

Fig. 16 Strict consensus of 12 most parsimonious trees
Tree length = 996 steps, consistency index = 0.3002 and retention index = 0.6715
Bremer indexes larger than 1 are indicated with numbers

possessing seven derived features shared with *Discoserra* and other chondrosteans, such as 1) the presence of an anterior junction of supraorbital and infraorbital canals between external nares (independently evolved in many early actinopterygians and holosteans), 2) presence of one or two supraorbitals, 3) absence of contribution of the maxilla to the posterior margin of the cheek, 4) presence of single dermopalatine, 5) absence of median gular, 6) presence of a complete set of dorsal ridge scales anterior to the dorsal fin, and 7) presence of ventral scutes anterior to the anal fin. Additionally, *Discoserra* is recovered as a sister taxon of *Ebenaqua*, *Bobasatrania* plus the remaining chondrosteans, supported by four character states: 1) presence of a dermopterotic (or supratemporal) not extending past the posterior margin of the parietal, 2) absence of the dermohyal, 3) absence of an expanded dorsal lamina of the maxilla, and 4) presence of multiple cheek bones bearing the preopercular canal.

The Triassic *Teffichthys*, *Louwoichthys*, *Luganoia* and *Venusichthys* are successively placed at the Neopterygii stem, and the sister group relationships between Holostei and Teleostei are supported within the Neopterygii crown. This topology is similar to those proposed by other recent analyses (Xu and Zhao, 2016; López-Arbarello and Sferco, 2018; Xu, 2020a, 2021; but see Giles et al., 2017).

5.3 Phylogenetic and ecological implications

Pteronisculus changae sp. nov. documents the second species of this genus from the early Middle Triassic (Anisian) Luoping Biota, and represents one of the youngest records of this genus, along with *P. nielseni* from the same biota. The recent finding adds new information to the morphological diversity of the genus (as listed above) and the taxonomic diversity of the Luoping Biota in the Middle Triassic Yangtze Sea, a part of the eastern Paleotethys Ocean. Outside of China, species of *Pteronisculus* are known only in the older (Early Triassic) marine deposits in Europe, Madagascar and North America. The successive discoveries of *P. nielseni* and *P. changae* indicate that *Pteronisculus* lived through the Early Triassic and survived at least until the early stage of the Middle Triassic. Based on this geological range and distribution of *Pteronisculus*, the Yangtze Sea in South China appears to be a refuge of this genus during the Middle Triassic.

The sister taxon relationships between *Pteronisculus* and *Cyranorhis* are proposed here for the first time. The later taxon lived in the Early Carboniferous, an important period for the early radiation of actinopterygians (Sallan, 2014; Friedman, 2015). Although *Pteronisculus* was known only in Early to Middle Triassic, its affinities to *Cyranorhis* indicate that the divergence between both taxa probably occurred as early as this period. *Pteronisculus* and *Cyranorhis* were traditionally placed in the ‘paleoniscoid’ families, the Palaeoniscidae (White, 1933) and Rhadinichthyidae (Lund and Poplin, 1997) respectively, but both families are likely paraphyletic. Recently, Romano et al. (2019) tentatively placed *Pteronisculus* into the Turseoidae, a family represented only by the Late Triassic *Turseodus* in USA before (Schaeffer, 1952, 1967), on the basis of their resemblances in the skull pattern and fins. However,

Turseodus remains poorly known in some phylogenetically important features (e.g., dermal bones in the snout region), and its detailed comparisons with *Pteronisculus* will be the subject of future studies. Based on the sister relationships between *Pteronisculus* and *Cyranorhis* proposed here, we tentatively place *Pteronisculus* into the Rhadinichthyidae.

The results of our phylogenetic analysis provide new insights into the phylogenetic relationships of 'platysomoid' actinopterygians. The Eurynotiformes (*Amphicentrum*, *Fouldenia* and *Styracopterus*) is recovered at the Actinopterygii stem, phylogenetically distant from other hypsisomatic fishes (*Discoserra*, *Ebenaqua* and *Bobasatrania*) that are recovered here as stem chondrosteans (rather than stem neopterygians; Giles et al., 2017; Argyriou et al., 2018). This renders to support a paraphyletic 'Platysomoidei'; the deep body form has independently evolved multiple times in the Carboniferous to Triassic actinopterygians (Sallan and Coates, 2013).

Results of our analysis support the historically prevalent hypothesis of the chondrostean affinities of birgeriiforms and saurichthyiforms. Argyriou et al. (2018), based on their studies of internal cranial anatomy of *Saurichthys*, proposed the sister group relationships between Birgeriiformes and Saurichthyiformes at the Actinopterygii stem. These sister group relationships, however, are not supported in our analysis, although we strictly followed Argyriou et al.'s (2018) codings for *Saurichthys* and *Birgeria* here. The differences between our and Argyriou et al.'s (2018) topologies are most likely due to minor revisions on a few character codings for several early actinopterygian taxa other than *Saurichthys* and *Birgeria* in our data matrix (see Supplementary Material on line).

The discovery of *P. changae* provides an important addition for investigating the trophic structure of the early Middle Triassic marine ecosystems in Luoping, eastern Yunnan. The previously known *P. nielseni* from the Luoping Biota represents one of the smallest members of the genus with a maximum total length of 127 mm (SL=102 mm), which is largely equal to some species from the Early Triassic of Madagascar. In comparison, other Early Triassic species (mainly from Europe) are significantly larger with a total length of 190–400 mm (Nielsen, 1942). *P. changae* has a maximum total length of 295 mm, 2.3 times as long as the coeval *P. nielseni*, representing the largest stem actinopterygian in the early Middle Triassic of China. Non-saurichthyid actinopterygians with a body length exceeding 200 mm are scarce in the Luoping biota; they were known only by the ionoscopiform halecomorph *Robustichthys* (Xu et al., 2014c; Xu, 2019) and colobodontid neopterygian *Feroxichthys* (Xu, 2020b). Among them, *Robustichthys* is likely a voracious and opportunistic predator and *Feroxichthys* a durophagous predator. The large body size and numerous forwardly-inclined and sharply-pointed teeth in the jaws of *P. changae* indicate that it is another predator in this biota. The teeth are relatively small and slender, lacking durophagous feeding adaptations. The elongated fusiform body form, long caudal peduncle, deeply forked caudal fin and deep pit-organs in the scales indicate that *P. changae* is a relatively fast swimmer (Schaeffer and Rosen, 1961; Webb, 1984; Montgomery et al., 2007). *P. changae* probably lived in the middle to top of the water

column, feeding on planktonic invertebrates and smaller or younger fishes, which are rich in the same marine ecosystems (Hu et al., 2011; Benton et al., 2013).

6 Conclusions

Studies of five well-preserved specimens recover a convincing new species of *Pteronisculus* from the Anisian Luoping Biota, which represents the largest stem actinopterygian fish in the early Middle Triassic of China. The new finding provides an important addition for our understanding of the taxonomic diversity and trophic structure of the early Middle Triassic marine ecosystems in the eastern Paleotethys Ocean. Phylogenetic study recovers *Pteronisculus* as a sister taxon of *Cyranorhis* at the Actinopterygii stem, and provides insights into the interrelationships of *Pteronisculus* and other actinopterygians. On the other hand, 'Platysomoidei' remains a paraphyletic group, and the historically alleged chondrostean affinities of birgeriiforms and saurichthyiforms cannot be excluded based on the current knowledge of the internal cranial anatomy for *Saurichthys*; further studies are still needed to reveal the evolutionary history of these specialized lineages of basal actinopterygians. The successive discoveries of *Pteronisculus nielseni* and *P. changae* sp. nov. from Luoping strongly support that *Pteronisculus* was not extinct at the end of the Early Triassic and the eastern Paleotethys Ocean could be a refuge for this genus during the early Middle Triassic.

Acknowledgments We thank Chang M. M. for all the constructive suggestions and discussions, Lü M. N. and Li Z. Y. for the specimen preparation, and Martha Richter and Carlo Romano for their valuable comments on an earlier version of this manuscript. We also greatly appreciate Martha Richter granting us access to comparative fossil materials in the Natural History Museum (London).

云南罗平中三叠世翼鳕属一新种及早期辐鳍鱼类系统发育关系

任 艺[1,2,3] 徐光辉[1,2]

(1 中国科学院古脊椎动物与古人类研究所，中国科学院脊椎动物演化与人类起源重点实验室 北京 100044)

(2 中国科学院生物演化与环境卓越创新中心 北京 100044)

(3 中国科学院大学 北京 100049)

摘要：辐鳍鱼亚纲是现存脊椎动物中最大的类群，包括腕鳍鱼次亚纲、辐鳍鱼次亚纲(包括软骨硬鳞类和新鳍鱼类)和亲缘关系密切的化石类群。已灭绝的翼鳕属(*Pteronisculus*)是隶属于辐鳍鱼亚纲的一个干群，包括产于马达加斯加、欧洲和北美下三叠统的11个种和中国中三叠统的一个种。根据滇东罗平中三叠世(安尼期)海相地层中发现的5块保存完好的化

石，命名翼鳕属一新种，张氏翼鳕(*Pteronisculus changae* sp. nov.)。这是翼鳕属在中三叠世的第二个确切种，最大体长达295 mm, 代表了罗平生物群中已知体型最大的辐鳍鱼亚纲干群物种。新种具有翼鳕属的独特衍征，泪骨具有牙齿，但它又有明显区别于本属其他种的自近裔特征，如间颞骨中部有一个内突起，21根上神经骨，83列侧线鳞。分支分析结果为早期辐鳍鱼类系统发育关系提供了新的见解，认为翼鳕属是*Cyranorhis*的姐妹群。根据体型和口缘牙齿等特征推测张氏翼鳕是一个快速游动的捕食者，以浮游无脊椎动物和体型较小的鱼类或鱼类幼体为食。作为翼鳕属最年轻的成员之一，张氏翼鳕的发现进一步表明翼鳕的多样性比我们过去认识的要高，古特提斯洋东缘可能是该属在中三叠世早期的避难所。

关键词：云南罗平，中三叠世，翼鳕属，辐鳍鱼类，系统发育

References

Argyriou T, Giles S, Friedman M et al., 2018. Internal cranial anatomy of Early Triassic species of †*Saurichthys* (Actinopterygii: †Saurichthyiformes): implications for the phylogenetic placement of †saurichthyiforms. BMC Evol Biol, 18: 161, doi: 10.1186/s12862-018-1264-4

Arratia G, 2009. Identifying patterns of diversity of the actinopterygian fulcra. Acta Zool Sup, 90: 220–235

Arratia G, Cloutier R, 1996. Reassessment of the morphology of *Cheirolepis canadensis* (Cheirolepididae: Actinopterygii). In: Schultze H P, Cloutier R eds. Devonian Fishes and Plants of Miguasha, Quebec, Canada. Munich: Verlag Dr. F. Pfeil. 165–197

Bartram A W H, 1975. The holostean fish genus *Ophiopsis* Agassiz. Zool J Linn Soc, 56: 183–205

Basden A M, Young G C, 2001. A primitive actinopterygian neurocranium from the Early Devonian of southeastern Australia. J Vert Paleont, 21: 754–766

Bender P A, 2002. A new late Permian ray-finned (actinopterygian) fish from the Beaufort Group, South Africa. Palaeont Afr, 38: 33–47

Bender P A, 2004. Late Permian actinopterygian (palaeoniscid) fishes from the Beaufort Group, South Africa: biostratigraphic and biogeographic implications. Coun Geosci Bull, 135: 1–84

Bender P A, 2005. A new deep-bodied late Permian actinopterygian fish from the Beaufort Group, South Africa. Palaeont Afr, 41: 7–22

Benton M J, Zhang Q Y, Hu S X et al., 2013. Exceptional vertebrate biotas from the Triassic of China, and the expansion of marine ecosystems after the Permo-Triassic mass extinction. Earth-Sci Rev, 125: 199–243

Choo B, 2011. Revision of the actinopterygian genus *Mimipiscis* (=*Mimia*) from the Upper Devonian Gogo Formation of western Australia and the interrelationships of the early Actinopterygii. Earth Env Sci Trans R Soc, 102: 77–104

Coates M I, 1999. Endocranial preservation of a Carboniferous actinopterygian from Lancashire, UK, and the interrelationships of primitive actinopterygians. Philos Trans R Soc B, 354: 435–462

Cope E D, 1887. Zittel's manual of palaeontology. Am Nat, 21: 1014–1019

Feldmann R M, Schweitzer C E, Hu S X et al., 2012. Macrurous Decapoda from the Luoping Biota (Middle Triassic) of China. J Paleont, 86: 425–441

Figueiredo F J D, Carvalho Bartira C M C, 2004. A new actinopterygian fish from the late Permian of the Parana basin, southern Brazil. Arq Mus Nac, 62: 531–547

Friedman M, 2015. The early evolution of ray-finned fishes. Palaeontology, 58(2): 213–228

Gardiner B G, 1966. Catalogue of Canadian fossil fishes. R Ontario Mus Univ Toronto, 68: 1–154

Gardiner B G, 1984. The relationships of the palaeoniscid fishes, a review based on new specimens of *Mimia* and *Moythomasia* from the Upper Devonian of western Australia. Bull Br Mus Nat Hist Geol, 37: 173–428

Gardiner B G, 1993. Osteichthyes: basal actinopterygians. In: Benton M J ed. The Fossil Record 2. London: Chapman and Hall. 611–619

Gardiner B G, Schaeffer B, 1989. Interrelationships of lower Actinopterygian fishes. Zool J Linn Soc, 97: 135–187

Gardiner B G, Schaeffer B, Masserie J A, 2005. A review of lower actinopterygian phylogeny. Zool J Linn Soc, 144: 511–525

Giles S, Xu G H, Near T J et al., 2017. Early members of 'living fossil' lineage imply later origin of modern ray-finned fishes. Nature, 549: 265–268

Grande L, Bemis W E, 1998. A comprehensive phylogenetic study of amiid fishes (Amiidae) based on comparative skeletal anatomy. An empirical search for interconnected patterns of natural history. Mem Soc Vert Paleont, 4: 1–690

Hamel M H, 2005. A new lower Actinopterygian from the early Permian of the Paraná Basin, Brazil. J Vert Paleont, 25:19–26

Hu S X, Zhang Q Y, Chen Z Q et al., 2011. The Luoping biota: exceptional preservation, and new evidence on the Triassic recovery from end-Permian mass extinction. Proc R Soc B, 278: 2274–2282

Hurley I A, Mueller R L, Dunn K et al., 2007. A new timescale for ray-finned fish evolution. Proc R Soc B, 274: 489–498

Lane J A, Ebert M, 2015. A taxonomic reassessment of *Ophiopsis* (Halecomorphi, Ionoscopiformes), with a revision of Upper Jurassic species from the Solnhofen Archipelago, and a new genus of Ophiopsidae. J Vert Paleont, 35: 1–23

Lehman J P, 1952. Etude complémentaire des poissons de l'Eotrias de Madagascar. Kungl Svenska Vetenska Handl, 4 Ser, 2: 1–201

López-Arbarello A, Sferco E, 2018. Neopterygian phylogeny: the merger assay. R Soc Open Sci, 5: 172337

López-Arbarello A, Sun Z Y, Sferco E et al., 2011. New species of *Sangiorgioichthys* Tintori and Lombardo, 2007 (Neopterygii, Semionotiformes) from the Anisian of Luoping (Yunnan Province, South China). Zootaxa, 2749: 25–39

Lu J S, Giles S, Friedman M, 2016. The oldest actinopterygian highlights the cryptic early history of the hyperdiverse ray-finned fishes. Curr Biol, 26: 1602–1608

Lund R, 2000. The new actinopterygian order Guildayichthyiformes from the Lower Carboniferous of Montana (USA). Geodiversitas, 22: 171–206

Lund R, Poplin C, 1997. The rhadinichthyids (paleoniscoid actinopterygians) from the Bear Gulch Limestone of Montana (USA, Lower Carboniferous). J Vert Paleont, 17: 466–486

Ma X Y, Xu G H, 2017. A new ionoscopiform fish (Holostei: Halecomorphi) from the Middle Triassic (Anisian) of Yunnan, China. Vert PalAsiat, 55: 92–106

Maisey J G, 1999. The supraotic bone in neopterygian fishes (Osteichthyes, Actinopterygii). Am Mus Novit, 3267:

1–52

Marramà G, Lombardo C, Tintori A et al., 2017. Redescription of '*Perleidus*' (Osteichthyes, Actinopterygii) from the Early Triassic of northwestern Madagascar. Riv Ital Paleont Stratigr, 123: 219–242

Mickle K E, 2018. A new lower actinopterygian fish from the Upper Mississippian Bluefield Formation of West Virginia, USA. PeerJ, 6: e5533

Mickle K E, Lund R, Grogan E D, 2009. Three new palaeoniscoid fishes from the Bear Gulch Limestone (Serpukhovian, Mississippian) of Montana (USA) and the relationships of lower actinopterygians. Geodiversitas, 31: 623–668

Montgomery J C, Baker C F, Carton A G, 1997. The lateral line can mediate rheotaxis in fish. Nature, 389: 960–963

Nielsen E, 1942. Studies on Trassic fishes from East Greenland I. *Glaucolepis* and *Boreosomus*. Medd Grønl, 146: 1–309

Patterson C, 1982. Morphology and interrelationships of primitive actinopterygian fishes. Am Zool, 22: 241–259

Pearson D M, 1982. Primitive bony fishes, with especial reference to *Cheirolepis* and palaeonisciform actinopterygians. Zool J Linn Soc, 74: 35–67

Pearson D M, Westoll T S, 1979. The Devonian actinopterygian *Cheirolepis* Agassiz. Trans R Soc Edinb, 70: 337–399

Piveteau J, 1934. Paléontologie de Madagascar, XXI. Les poissons du Trias inferieur. Contribution à l'étude des Actinoptérygiens. Ann Paléont, 23: 81–180

Poplin C M, Lund R, 2000. Two new deep-bodied palaeoniscoid actinopterygians from Bear Gulch (Montana, USA, Lower Carboniferous). J Vert Paleont, 20: 428–449

Poplin C M, Lund R, 2002. Two carboniferous fine-eyed palaeoniscoids (pisces, actinopterygii) from bear gulch (USA). J Paleont, 76: 1014–1028

Romano C, López-Arbarello A, Ware D et al., 2019. Marine Early Triassic Actinopterygii from the Candelaria Hills (Esmeralda County, Nevada, USA). J Paleont, 93: 971–1000

Romer A S, 1945. Vertebrate Paleontology. Chicago: University Chicago Press. 1–687

Sallan L C, 2014. Major issues in the origins of ray-finned fish (Actinopterygii) biodiversity. Biol Rev, 89: 950–971

Sallan L C, Coates M I, 2013. Styracopterid (Actinopterygii) ontogeny and the multiple origins of post-Hangenberg deep-bodied fishes. Zool J Linn Soc, 169: 156–199

Schaeffer B, 1952. The palaeoniscoid fish *Turseodus* from the Upper Triassic Newark Group. Am Mus Novit, 1581: 1–24

Schaeffer B, 1967. Late Triassic fishes from the western United States. Bull Am Mus Nat Hist, 35: 285–342

Schaeffer B, Mangus M, 1976. An Early Triassic fish assemblage from British Columbia. Bull Am Mus Nat Hist, 156: 127–216

Schaeffer B, Rosen D E, 1961. Major adaptive levels in the evolution of the Actinopterygian feeding mechanism. Am Zool, 1: 187–204

Schultze H P, 1966. Morphologische und histologische Untersuchungen an Schuppen Mesozoicher Actinopterygier (übergang von Ganoid zu Rundshuppen). Neues Jahrb Geol Palaontol Abh, 126: 243–259

Schultze H P, 2015. Scales, enamel, cosmine, ganoine, and early Osteichthyans. C R Palevol, 15: 83–102

Schultze H P, Bardack D, 1987. Diversity and size changes in palaeonisciform fishes (Actinopterygii, Pisces) from the Pennsylvanian Mazon Creek fauna, Illinois, U.S.A. J Vert Paleont, 7: 1–23

Su D Z, 1959. Triassic fishes from Kueichow, Southwest China. Vert PalAsiat, 3: 205–210

Sun Z Y, Tintori A, Jiang D Y et al., 2009. A new perleidiform (Actinopterygii, Osteichthyes) from the middle Anisian (Middle Triassic) of Yunnan, South China. Acta Geol Sin, 83: 460–470

Sun Z Y, Lombardo C, Tintori A et al., 2015. A new species of *Altisolepis* (Peltopleuriformes, Actinopterygii) from the Middle Triassic of southern China. J Vert Paleont, 35: e909819

Sun Z Y, Tintori A, Xu Y Z et al., 2016. A new non-parasemionotiform order of the Halecomorphi (Neopterygii, Actinopterygii) from the Middle Triassic of Tethys. J Syst Palaeont, 15: 223–240

Swartz B A, 2009. Devonian actinopterygian phylogeny and evolution based on a redescription of *Stegotrachelus finlayi*. Zool J Linn Soc, 56: 750–784

Tintori A, Sun Z Y, Lombardo C et al., 2007. New specialized basal neopterygians (Actinopterygii) from Triassic of the Tethys Realm. Geol Insubrica, 10: 13–20

Tintori A, Sun Z Y, Lombardo C et al., 2010. A new basal neopterygian from the Middle Triassic of Luoping County (South China). Riv Ital Paleont Stratigr, 116: 161–172

Wagner A, 1863. Monographie der fossilen Fische aus den Lithographischen Schiefern Bayerns. Abh K Bayer Akad Wiss Math Phys, 9: 611–748

Wang N Z, Dong Z Z, 1989. Discovery of Late Silurian microfossils of Agnatha and fishes from Yunnan, China. Acta Palaeont Sin, 28: 192–206

Webb P W, 1984. Body form, locomotion and foraging in aquatic vertebrates. Am Zool, 24: 107–120

Wen W, Zhang Q Y, Hu S X et al., 2012. A new basal actinopterygian fish from the Anisian (Middle Triassic) of Luoping, Yunnan Province, Southwest China. Acta Palaeont Pol, 57: 149–160

Wen W, Zhang Q Y, Hu S X et al., 2013. Coelacanths from the Middle Triassic Luoping Biota, Yunnan, South China, with the earliest evidence of ovoviviparity. Acta Palaeont Pol, 58: 175–193

Wen W, Hu S X, Zhang Q Y et al., 2019. A new species of *Platysiagum* from the Luoping Biota (Anisian, Middle Triassic, Yunnan, South China) reveals the relationship between Platysiagidae and Neopterygii. Geol Mag, 156: 669–682

Westoll T S, 1944. The Haplolepidae, a new family of Late Carboniferous bony fishes—a study in taxonomy and evolution. Bull Am Mus Nat Hist, 83: 1–121

White E I, 1933. New Triassic palaeoniscids from Madagascar. Ann Mag Nat Hist, 10: 118–128

Wilson C D, Pardo J D, Anderson J S, 2018. A primitive actinopterygian braincase from the Tournaisian of Nova Scotia. R Soc Open Sci, 5: 171727

Wu F X, Sun Y L, Xu G H et al., 2011. New saurichthyid actinopterygian fishes from the Anisian (Middle Triassic) of southwestern China. Acta Palaeont Pol, 56: 581–614

Xu G H, 2019. Osteology and phylogeny of *Robustichthys luopingensis*, the largest holostean fish in the Middle Triassic. PeerJ, 7: e7184

Xu G H, 2020a. A new species of *Luganoia* (Luganoiidae, Neopterygii) from the Middle Triassic Xingyi Biota, Guizhou, China. Vert PalAsiat, 58: 267–282

Xu G H, 2020b. *Feroxichthys yunnanensis* gen. et sp. nov. (Colobodontidae, Neopterygii), a large durophagous predator from the Middle Triassic (Anisian) Luoping Biota, eastern Yunnan, China. PeerJ, 8: e10229

Xu G H, 2021. A new stem-neopterygian fish from the Middle Triassic (Anisian) of Yunnan, China, with a reassessment of

the relationships of early neopterygian clades. Zool J Linn Soc, 191: 375–394

Xu G H, Gao K Q, 2011. A new scanilepiform from the Lower Triassic of northern Gansu Province, China, and phylogenetic relationships of non-teleostean Actinopterygii. Zool J Linn Soc, 161: 595–612

Xu G H, Ma X Y, 2016. A Middle Triassic stem-neopterygian fish from China sheds new light on the peltopleuriform phylogeny and internal fertilization. Sci Bull, 61: 1766–1774

Xu G H, Ma X Y, 2018. Redescription and phylogenetic reassessment of *Asialepidotus shingyiensis* (Holostei: Halecomorphi) from the Middle Triassic (Ladinian) of China. Zool J Linn Soc, 184: 95–114

Xu G H, Wu F X, 2012. A deep-bodied ginglymodian fish from the Middle Triassic of eastern Yunnan Province, China, and the phylogeny of lower neopterygians. Chinese Sci Bull, 57: 111–118

Xu G H, Zhao L J, 2016. A Middle Triassic stem-neopterygian fish from China shows remarkable secondary sexual characteristics. Sci Bull, 61: 338–344

Xu G H, Gao K Q, Finarelli J A, 2014a. A revision of the Middle Triassic scanilepiform fish *Fukangichthys longidorsalis* from Xinjiang, China, with comments on the phylogeny of the Actinopteri. J Vert Paleont, 34: 747–759

Xu G H, Shen C C, Zhao L J et al., 2014b. *Pteronisculus nielseni* sp. nov., a new stem-actinopteran fish from the Middle Triassic of Luoping, Yunnan Province, China. Vert PalAsiat, 52: 364–380

Xu G H, Zhao L J, Coates M I, 2014c. The oldest ionoscopiform from China sheds new light on the early evolution of halecomorph fishes. Biol Lett, 10: 20140204

Zhang Q Y, Zhou C Y, Lü T et al., 2009. A conodont-based Middle Triassic age assignment for the Luoping Biota of Yunnan, China. Sci China Ser D, 52: 1673–1678

Zhang Q Y, Hu S X, Wen W et al., 2015. Research achievements and prospect on the Luoping Biota: according to 1:50000 regional geological survey and achievement of specific study for Luoping, Guishan, Datong, Pengzha, Yunnan. Geol Surv China, 2: 24–32

Zhu M, Yu X B, Janvier P, 1999. A primitive fossil fish sheds light on the origin of bony fishes. Nature, 397: 607–610